MCB
Journals.ASM.org

Downregulation of STRA6 in Adipocytes and Adipose Stromovascular Fraction in Obesity and Effects of Adipocyte-Specific STRA6 Knockdown *In Vivo*

Laura Zemany,[a] Bettina J. Kraus,[a]* Julie Norseen,[a] Tsugumichi Saito,[a]* Odile D. Peroni,[a] Randy L. Johnson,[b] Barbara B. Kahn[a]

Division of Endocrinology, Diabetes, and Metabolism, Department of Medicine, Beth Israel Deaconess Medical Center and Harvard Medical School, Boston, Massachusetts, USA[a]; Department of Biochemistry and Molecular Biology, M. D. Anderson Cancer Center, Houston, Texas, USA[b]

To investigate the mechanisms by which elevated retinol-binding protein 4 (RBP4) causes insulin resistance, we studied the role of the high-affinity receptor for RBP4, STRA6 (stimulated by retinoic acid), in insulin resistance and obesity. In high-fat-diet-fed and *ob*/*ob* mice, STRA6 expression was decreased 70 to 95% in perigonadal adipocytes and both perigonadal and subcutaneous adipose stromovascular cells. To determine whether downregulation of STRA6 in adipocytes contributes to insulin resistance, we generated adipose-Stra6$^{-/-}$ mice. Adipose-Stra6$^{-/-}$ mice fed chow had decreased body weight, fat mass, leptin levels, insulin levels, and adipocyte number and increased expression of brown fat-selective markers in white adipose tissue. When fed a high-fat diet, these mice had a mild improvement in insulin sensitivity at an age when adiposity was unchanged. STRA6 has been implicated in retinol uptake, but retinol uptake and the expression of retinoid homeostatic genes (encoding retinoic acid receptor β [RARβ], CYP26A1, and lecithin retinol acyltransferase) were not altered in adipocytes from adipose-Stra6$^{-/-}$ mice, indicating that retinoid homeostasis was maintained with STRA6 knockdown. Thus, STRA6 reduction in adipocytes in adipose-Stra6$^{-/-}$ mice fed chow resulted in leanness, which may contribute to their increased insulin sensitivity. However, in wild-type mice with high-fat-diet-induced obesity and in *ob*/*ob* mice, the marked downregulation of STRA6 in adipocytes and adipose stromovascular cells does not compensate for obesity-associated insulin resistance.

Three hundred fifty million people worldwide have diabetes (1), and the impact will be staggering if we do not develop more effective methods for early detection and treatment. Serum retinol-binding protein 4 (RBP4) is elevated in humans and rodents with insulin resistance and type 2 diabetes (2–4), and data suggest that it may play a causative role (4, 5). Injection of purified RBP4 or overexpression of RBP4 in mice causes insulin resistance (4). Furthermore, a gain-of-function polymorphism in the RBP4 promoter is associated with an 80% increased risk of developing diabetes in humans (5). In addition, epidemiologic studies in several ethnic backgrounds indicate that elevated RBP4 is an early marker of prediabetes (6) and metabolic syndrome (7, 8) and is associated with a 3.6-fold increased risk of myocardial infarction (9).

The mechanisms by which RBP4 causes insulin resistance and whether the actions of RBP4 depend on a receptor are questions of high interest in the field. STRA6 is a high-affinity cell surface receptor for RBP4 that mediates vitamin A uptake (10). STRA6 is highly expressed in blood-organ barriers and in the brain, eye, kidney, testis, and female reproductive tract, and it is absent from the liver (11). STRA6 is upregulated in some tumors, and its expression can be induced by retinoids and increased Wnt-1 expression in mammary epithelial cells (12). RBP4 mediates insulin resistance through STRA6-independent (13, 14) and STRA6-dependent pathways (15, 16). Genetic data show that single nucleotide polymorphisms in STRA6 are associated with type 2 diabetes (17), raising the possibility that STRA6 plays an important role in altered metabolic states. In addition, STRA6 has been proposed to play a role in insulin resistance on the basis of data from a total-body STRA6 knockout mouse (18), although the contribution of STRA6 in adipose tissue has not been studied. Thus, we sought to determine whether STRA6 is regulated in insulin target tissues in obesity and diabetes.

Although STRA6 mediates retinol uptake from RBP4 (10), the contribution of STRA6 to retinoid homeostasis is still under investigation. Mutations of STRA6 in humans are associated with Matthew-Wood syndrome, which is characterized by pleiotropic, multisystem malformations that include cardiac deformities and ocular defects (19–22), which are consistent with abnormalities seen in altered vitamin A metabolism. Studies with STRA6 null mice show that STRA6 is important for retinol uptake and processing of retinol by the retinal pigment epithelium, but STRA6 is not the only pathway for retinol uptake in the retinal pigment epithelium (23). Although the liver is the main retinol storage site, white adipose tissue contains ~15% of the retinoid stores in the adult rat, indicating that adipose tissue is important in retinoid storage and metabolism (24), and its role could be even greater in obesity because of the expanded adipose mass. The importance of STRA6-mediated retinol uptake in adipose tissue retinoid metab-

Received 26 August 2013 **Returned for modification** 17 September 2013
Accepted 6 January 2014

Published ahead of print 13 January 2014

Address correspondence to Barbara B. Kahn, bkahn@bidmc.harvard.edu.

* Present address: Bettina J. Kraus, University Hospital Würzburg, Department of Internal Medicine I, Würzburg, Germany; Tsugumichi Saito, Department of Medicine and Molecular Science, Gunma University Graduate School of Medicine, Maebashi, Gunma, Japan.

Supplemental material for this article may be found at http://dx.doi.org/10.1128/MCB.01106-13.

doi:10.1128/MCB.01106-13

olism is unknown since tissues can acquire retinoids from several sources, including retinol-RBP4, retinoic acid, and retinyl esters in lipoproteins (25, 26).

Here we determined STRA6 expression in multiple tissues, including classic insulin target tissues, in lean and obese mice. We found a striking downregulation in adipocytes but not in muscle, the major tissue for insulin-stimulated glucose uptake. Given the downregulation in adipose tissue and the critical role that adipose tissue plays in the regulation of energy homeostasis and systemic insulin sensitivity (27), we targeted STRA6 expression specifically in adipocytes in mice to determine the importance of adipocyte-STRA6 in glucose homeostasis, obesity, and retinoid metabolism.

MATERIALS AND METHODS

Animals for STRA6 tissue distribution. For diet-induced obesity, male C57BL/6 mice were purchased at 10 weeks of age from The Jackson Laboratory, where they were fed a control diet (10% of calories from fat; Research Diet; D12450B) or a high-fat diet (60% of calories from fat; Research Diet; D12492). Upon arrival, they were switched to a chow (17% of calories from fat; Lab Diet; 5008) or high-fat (55% of calories from fat; Harlan Teklad; 93075) diet with *ad libitum* access to food and water and euthanized 4 weeks after their arrival. Female *ob*/*ob* mice and their lean littermates fed a chow diet were purchased from The Jackson Laboratory at 10 weeks of age and euthanized 3 weeks after their arrival. Mice for tissue distribution studies were maintained in a temperature-controlled environment with a 14-h light and10-h dark cycle.

Generation of adipose-Stra6$^{-/-}$ mice. STRA6 flox/flox mice were generated by inserting *loxP* sites into the first intron and into the 3′ untranslated region (UTR). *loxP*-FRT3-*puro*-FRT3 was inserted at the 5′ *loxP* site, and internal ribosome entry site (IRES)-*lacZ*-FRT-*neo*-FRT-*loxP* was inserted at the 3′ *loxP* site. The FRT3-*puro*-FRT3 and FRT-*neo*-FRT cassettes were removed by mating chimeras with Flpe mice, and germ line transmission was obtained. STRA6 flox/flox mice were on a mixed C57BL/6, 129SvEv, and CD1 background. Adiponectin Cre mice on a predominantly C57BL/6 background (28) were generously provided by Evan Rosen, Beth Israel Deaconess Medical Center, Harvard Medical School, and were used to generate adipocyte-specific deletion as previously described (29). Our breeding demonstrated that the adiponectin-Cre construct was inserted into the same chromosome on which STRA6 is located (chromosome 9). Therefore, mice were generated by crossing (Cre^{+}/flox^{+})/(Cre^{-}/flox^{-}) or (Cre^{+}/flox^{-})/(Cre^{-}/flox^{+}) male mice with female mice heterozygous for flox. Primers A and B were used to detect the STRA6 flox/flox allele, and primers C and D were used to detect the recombined allele. After demonstrating that the STRA6 flox/flox mice had no metabolic phenotype, we used the STRA6 flox/flox mice as controls for all further studies. The following primers were used to genotype the mice: genotyping primer A, 5′-CCTAAAGCATGACACAGGGC-3′; genotyping primer B, 5′-TACCGACAGTGAAGCCAGG-3′; genotyping primer C, 5′-AGGAGGGTCCTTGGAGGATA-3′; genotyping primer D, 5′-GTAGCCTGGTGGACAAGCAT-3′.

Mice were housed three or four per cage with *ad libitum* access to food and water, and adipose-Stra6$^{-/-}$ mice and their controls were maintained on a 12-h light and 12-h dark cycle. Mice were fed a standard chow diet (15 IU vitamin A/g and 17% of calories from fat; Lab Diet; 5008) or a high-fat diet. At 5 weeks of age, high-fat-diet-fed mice were fed a high-fat diet containing 4 IU vitamin A/g and 60% of the calories from fat (Research Diet; D12492), and at 8 weeks of age, they were switched to a high-fat diet containing 27 IU vitamin A/g and 55% of the calories from fat (Harlan Teklad; 93075), as the latter diet results in a higher degree of insulin resistance and obesity in wild-type mice. All aspects of animal care were approved by the Institutional Animal Care and Use Committee of the Beth Israel Deaconess Medical Center and Harvard Medical School.

Body weight and composition. Body weights were measured weekly. Body composition was determined by dual-energy X-ray absorptiometry (DEXA; Lunar PIXIMUS densitometer; GE Medical Systems) in mice anesthetized with a mixture of isoflurane (3%) and oxygen (97%) with a pressurized vaporizer. In female mice, perigonadal adipose tissue was defined as the intra-abdominal visceral depots attached to both horns of the uterus up to the ovaries. In male mice, perigonadal adipose tissue was defined as the prominent intra-abdominal visceral depots attached to the testicles. In both genders, subcutaneous white adipose tissue was defined as the superficial white adipose tissue between the skin and muscle fascia from the midline of the abdomen (abdominal belt) to the spine. For fat weights and adipocyte numbers, bilateral depots were used.

GTTs and ITTs. For glucose tolerance tests (GTTs) and insulin tolerance tests (ITTs), the food was removed at 8:00 a.m. for 5 h. GTTs were performed by the intraperitoneal (i.p.) injection of glucose at 1 g/kg of body weight. ITTs were performed by the i.p. injection of recombinant regular human insulin (Humulin; Lilly) at a dose of 0.5 to 0.7 U/kg of body weight. Blood glucose was measured at the indicated time points (One-Touch Ultra glucometer).

Indirect calorimetry. Animals were individually housed in metabolic chambers on a 12-h light and 12-h dark cycle. Metabolic measurements (oxygen consumption, locomotor activity, and food intake) were obtained with an indirect calorimetry system (Comprehensive Lab Animal Monitoring System [CLAMS]; Columbia Instruments). The CLAMS studies were performed at the NeuroBehavior Laboratory at the Harvard NeuroDiscovery Center.

Chemistries. Mice were bled either in the fed state in the morning (8 a.m. to 10 a.m.) or 5 h after the removal of food. Blood collections were performed by tail vein bleeding. Leptin and insulin levels were determined by enzyme-linked immunosorbent assay (Crystal Chem).

Quantitative PCR. Tissues were snap-frozen in liquid nitrogen and stored at −80°C prior to processing. RNA was extracted with TRI Reagent (Molecular Research Center). For adipose tissue samples from the adipose-Stra6$^{-/-}$ mice, an RNeasy kit (Qiagen) was used for further RNA purification. cDNA was generated with random hexamers (Advantage RT-for-PCR kit; Clontech). Quantitative real-time PCR was performed in a 7900 HT thermocycler (Applied Biosystems) with TaqMan universal Master Mix, Solaris Master Mix, or SYBR green PCR Master Mix (Applied Biosystems). TaqMan primers-probes were used to obtain the data in Fig. 2E and F. For TaqMan analysis, the primer-probe set used (12) included STRA6 forward (5′-AGCCAAGTCAGACTCCAAGAG-3′), STRA6 reverse (5′-CAGAGAGCACACTAACTTCTTTCA-3′), and STRA6 FAM (5′-CCCCACTGAGCTGCCCTCTCC-3′), and a commercially available primer probe was used for 18S rRNA (Applied Biosystems; 4310893E). Solaris primers-probes were used for RBP4 receptor 2 (RBPR2) measurements (RBPR2, 74152; actin, 11461; TATA-binding protein [TBP], 21374). All other measurements were performed with SYBR green. For the sequences of the primers used, see Table S1 in the supplemental material or references 30 to 32.

Western blotting. Serum was diluted 30-fold in a lysis buffer (20 mM Tris-Cl, 5 mM EDTA, 10 mM $Na_4P_2O_7$, 100 mM NaF, 1% NP-40, 6.7 μg/ml aprotinin, 6.7 μg/ml leupeptin, 1 mM phenylmethylsulfonyl fluoride, 2 mM Na_3VO_4). Samples were boiled for 5 min, and proteins were separated by 18% SDS-polyacrylamide gel electrophoresis. Mouse RBP4 was detected with an anti-human RBP4 polyclonal antibody (Dako; catalog number A0040) at a 1:500 dilution and a horseradish peroxidase-conjugated anti-rabbit secondary antibody at a 1:1,000 dilution. Transthyretin (TTR) was detected with an anti-human TTR polyclonal antibody that also recognizes mouse TTR (Dako; catalog number A0002). Bands were visualized with enhanced-chemiluminescence reagent (Amersham Life Sciences) and quantified with ImageQuant TL (GE Healthcare).

Adipocyte isolation and cell number determination. Adipocytes were isolated from adipose tissue as previously described (33). Briefly, perigonadal or subcutaneous adipose tissue was digested with collagenase (1 mg/ml) at 37°C in Krebs-Ringer-HEPES buffer (pH 7.4) with 3% bovine serum albumin and 200 nM adenosine. Cells were filtered through a

mesh and separated by spinning the suspension through dinonyl phthalate oil. After centrifugation, the adipocyte fraction and the pelleted stromovascular fraction (SVF) were transferred to TRI Reagent for RNA extraction. A small piece of adipose tissue was fixed in osmium, and cell size and number were determined in a Coulter counter as previously described (33, 34).

Glucose transport in isolated adipocytes. Glucose transport studies were performed as previously described (35). Isolated perigonadal adipocytes were incubated for 30 min in the absence (basal) or presence (insulin stimulated) of insulin at the indicated concentrations. [U-^{14}C]-glucose was then added, the mixture was incubated for 30 min, and the reaction was terminated by spinning the suspension through dinonyl phthalate oil.

Retinol uptake. Human retinol-bound RBP4 (holo-RBP4) was expressed in *Escherichia coli* and purified as described previously (4, 14). The endotoxin level of the protein was less that 0.001 endotoxin U/μg. Retinol-free RBP4 (apo-RBP4) was generated by stripping off the retinol from holo-RBP4 by incubating holo-RBP4 with 40% butanol–60% diisopropyl ether as previously described (14). Apo-RBP4 was reloaded with retinol (10-fold molar excess) by the addition of a mixture of unlabeled retinol and [^{3}H]retinol {American Radiolabeled Chemical; [15-^{3}H(N)retinol; catalog no. ART 0556}, and unbound retinol was removed with dextran-coated charcoal. The quality of the [^{3}H]retinol-RBP4 was confirmed by fluorescence spectrometry (14). Retinol uptake studies were performed with isolated perigonadal adipocytes by incubating cells with [^{3}H]retinol-RBP4 for the indicated duration at the indicated concentration. The dialysate buffer was used as a control in the experiments. After incubation, the cells were spun through dinonyl phthalate oil and collected in scintillation tubes. Radioactivity was measured by scintillation counting. Counts were normalized per adipocyte, and retinol uptake is expressed in femtomoles per cell.

Statistics. All values are presented as the mean ± the standard error of the mean (SEM). A P value of <0.05 was considered significant. Statistical analysis was performed with Student's two-tailed t test, one-way analysis of variance (ANOVA), or two-way ANOVA, as appropriate. GraphPad Prism 5 was used for analysis.

RESULTS

STRA6 tissue distribution. STRA6 was highly expressed in the brain and eye and absent from the liver in male mice on a chow diet, consistent with previous studies (10, 11) (Fig. 1A). Kidney tissue was chosen as the reference for the graphs in Fig. 1 and 2 because of its intermediate level of expression. Expression in muscle was relatively low, with no significant differences between the different skeletal muscle types studied, including oxidative (soleus), glycolytic (tibialis), and mixed (gastrocnemius) muscles. In mice fed a chow diet, STRA6 expression was higher in subcutaneous white adipose tissue than in muscle, brown adipose tissue, and perigonadal adipose tissue. STRA6 expression in perigonadal white adipose tissue was similar to that in muscle.

To determine the regulation of STRA6 in insulin-resistant states and obesity, we measured STRA6 expression in mice with high-fat-diet-induced insulin resistance (Fig. 1B). As expected, the body weights of C56BL/6 mice fed a high-fat diet for 2 months were increased (Fig. 1C), and high-fat-diet-fed mice had elevated glucose, insulin, and serum RBP4 levels (Fig. 1D to F). ITTs also showed an elevated initial glucose level and an impaired response to insulin (Fig. 1G and H). In high-fat-diet-fed mice, STRA6 expression was still highest in the eye and brain, intermediate in the kidney, and low in muscle and adipose tissues (Fig. 1B). STRA6 expression was not present in the livers of lean mice and was not induced by a high-fat diet. In contrast to the 6-fold higher STRA6 expression in subcutaneous white adipose tissue compared to that in perigonadal white adipose tissue and muscles in mice fed a chow diet in high-fat-diet-fed mice, STRA6 expression in brown adipose tissue and white adipose tissue was lower than in muscle. In high-fat-diet-fed mice, STRA6 mRNA in subcutaneous white adipose tissue was 95% lower than its expression in the kidney, whereas STRA6 expression in subcutaneous white adipose tissue was comparable to that in the kidney in mice fed a chow diet.

We also determined whether STRA6 tissue distribution is altered in the *ob*/*ob* mouse, a genetic model of obesity and insulin resistance due to leptin deficiency. As expected, *ob*/*ob* mice were obese and had hyperglycemia and severe hyperinsulinemia (Fig. 2A to C). Serum RBP4 was elevated 1.7-fold in *ob*/*ob* mice (Fig. 2D). In lean female mice that were littermates of *ob*/*ob* mice (Fig. 2E), STRA6 tissue distribution was similar to that found in male mice (Fig. 1A). STRA6 expression in *ob*/*ob* mice was highest in the eye and brain (Fig. 2F), as was seen in lean and high-fat-diet-fed mice. However, in contrast to lean mice and in parallel with high-fat-diet-fed mice, STRA6 expression in adipose tissue was lower in all fat depots, including subcutaneous fat, compared to skeletal muscle. In subcutaneous white adipose tissue from lean mice, STRA6 levels were similar to those in the kidney, whereas the levels were >95% lower than those in the kidney in *ob*/*ob* mice.

Regulation of STRA6 in adipose fractions. Emerging evidence indicates that not all adipose tissue depots contribute equally to the development of insulin resistance (36). Therefore, we studied the effects of a high-fat diet on STRA6 expression in subcutaneous and perigonadal adipose tissue depots. We found that STRA6 was 6.5-fold lower in the perigonadal adipose tissue of high-fat-diet-fed mice than in that of chow-fed controls (Fig. 3A) and tended to be decreased in subcutaneous fat (Fig. 3B).

Since adipose tissue is composed of both adipocytes and stromovascular cells, we determined in which fraction STRA6 is expressed. In the perigonadal adipose tissue of control mice fed a chow diet, STRA6 expression was similar in adipocytes and the SVF (Fig. 3C). In contrast, in the subcutaneous adipose tissue of mice fed a chow diet, STRA6 expression in the SVF was higher than in adipocytes (Fig. 3D). Similarly, in the lean controls for *ob*/*ob* mice, STRA6 expression was comparable in adipocytes and the SVF in perigonadal fat, whereas in the subcutaneous depot, STRA6 expression was greater in the SVF than in the adipocyte fraction (Fig. 3E and F).

In high-fat-diet-fed mice, STRA6 expression was downregulated in isolated perigonadal adipocytes and there was a strong tendency for downregulation in the SVF from perigonadal fat ($P = 0.07$) (Fig. 3C). In contrast, in the subcutaneous fat of these mice, there was no downregulation and a tendency toward an increase in adipocytes, and STRA6 was downregulated 5.7-fold in the SVF from the same subcutaneous fat pads (Fig. 3D). Similar to the high-fat model, in *ob*/*ob* mice, STRA6 was decreased 17-fold in perigonadal adipocytes and 3.6-fold in the SVF from perigonadal fat (Fig. 3E). In subcutaneous fat of *ob*/*ob* mice, STRA6 was downregulated 4-fold in the stromovasculature but unchanged in the adipocyte fraction (Fig. 3F). Therefore, in these models of diet-induced and genetic obesity, there was a consistent decrease in STRA6 expression in perigonadal adipocytes and in the SVF from both perigonadal and subcutaneous fat.

In high-fat-diet-fed mice, unlike the downregulation of STRA6 in perigonadal and subcutaneous fat, STRA6 expression was not altered in brown adipose tissue or in skeletal (glycolytic, oxidative)

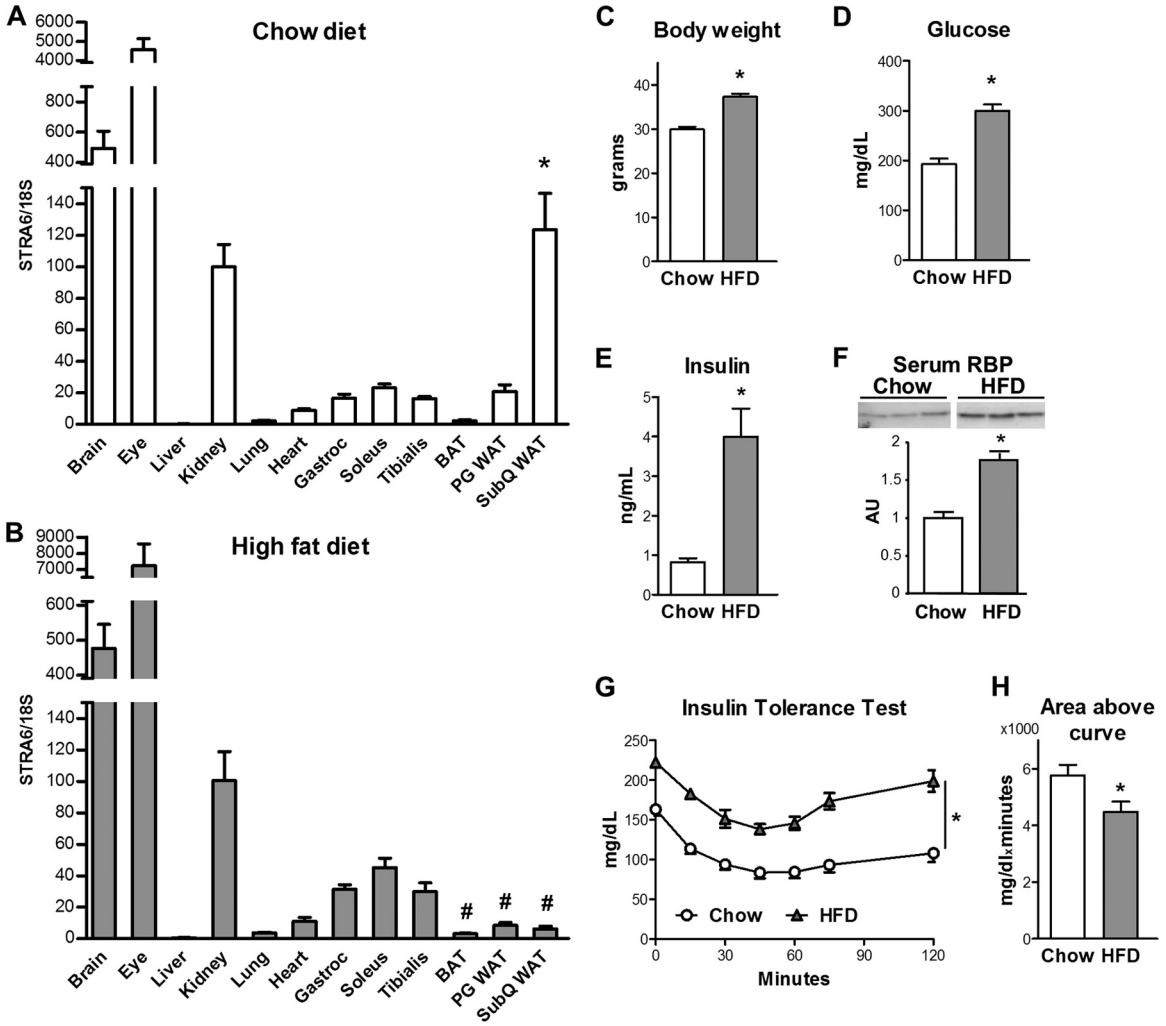

FIG 1 Tissue STRA6 distribution and metabolic characteristics of chow-fed and high-fat-diet-fed mice. (A) STRA6 mRNA expression in male C57BL/6 mice fed a chow diet. *, $P < 0.05$ versus heart, skeletal muscles, and other fat depots. (B) STRA6 mRNA expression in male C57BL/6 mice fed a high-fat diet (HFD). #, $P < 0.05$ versus all skeletal muscles. All data are expressed relative to levels in kidney in that group of mice and are normalized to 18S rRNA. Analysis was performed by ANOVA comparing skeletal muscles, heart, and fat depots. (C to F) Body weights and fed glucose, fed insulin, and serum RBP4 levels of 3-month-old male C57BL/6 mice fed chow and high-fat diets. *, $P < 0.05$ versus the control. (G and H) Insulin tolerance and area above the curve during an ITT (0.7 mU/g body weight) 5 h after food removal. *, $P < 0.05$ versus the control. Results represent five to eight animals per group. Data are expressed as mean ± SEM.

or cardiac muscle (Fig. 3G and H). In contrast to the high-fat diet model, STRA6 expression was increased 4.7-fold in brown adipose tissue and increased 1.9-fold in the soleus muscles of *ob*/*ob* mice (Fig. 3I and J). This coordinate regulation may reflect the fact that brown fat precursor cells express myogenic genes (37) and brown adipose tissue and skeletal muscle arise from *myf5*-expressing precursor cells (38).

STRA6 expression in white adipose tissue was calculated by using a standard curve because the expression of the housekeeping genes for cyclophilin, TBP, and 18S rRNA was altered with obesity (Fig. 4A to D). It is well known that the gene for glyceraldehyde 3-phosphate dehydrogenase, which is often used as a housekeeping gene, is highly upregulated in adipose tissue in obese rodents (39) and humans (40) and is downregulated in obese subjects with type 2 diabetes mellitus (40). The housekeeping genes were less variable in brown adipose tissue and skeletal and cardiac muscles of high-fat-diet-fed mice (Fig. 4E). In muscle from high-fat-diet-fed mice, STRA6 was normalized to TBP (Fig. 3H), since TBP expression in these tissues was not altered with high-fat feeding (Fig. 4E). The results for STRA6 expression relative to TBP in muscle were comparable to those measured with TaqMan primers and expressed relative to 18S rRNA in the muscles of a separate set of animals (data not shown).

Generation of adipose-Stra6$^{-/-}$ mice. Since STRA6 was decreased in perigonadal adipocytes in two models of insulin resistance, we determined the role of STRA6 in adipocytes in insulin resistance and glucose homeostasis by targeting the expression of STRA6 specifically in adipocytes. Adipose-Stra6$^{-/-}$ mice were born at the expected Mendelian frequency. A PCR assay performed on DNA with primers flanking the first *loxP* site (primers A and B) showed that ~50% of the adipocyte DNA from adipose-Stra6$^{-/-}$ mice was not recombined, indicating that 50% of the DNA had been recombined (Fig. 5A). We then determined that STRA6 was deleted only from adipocytes (primers C and D). The

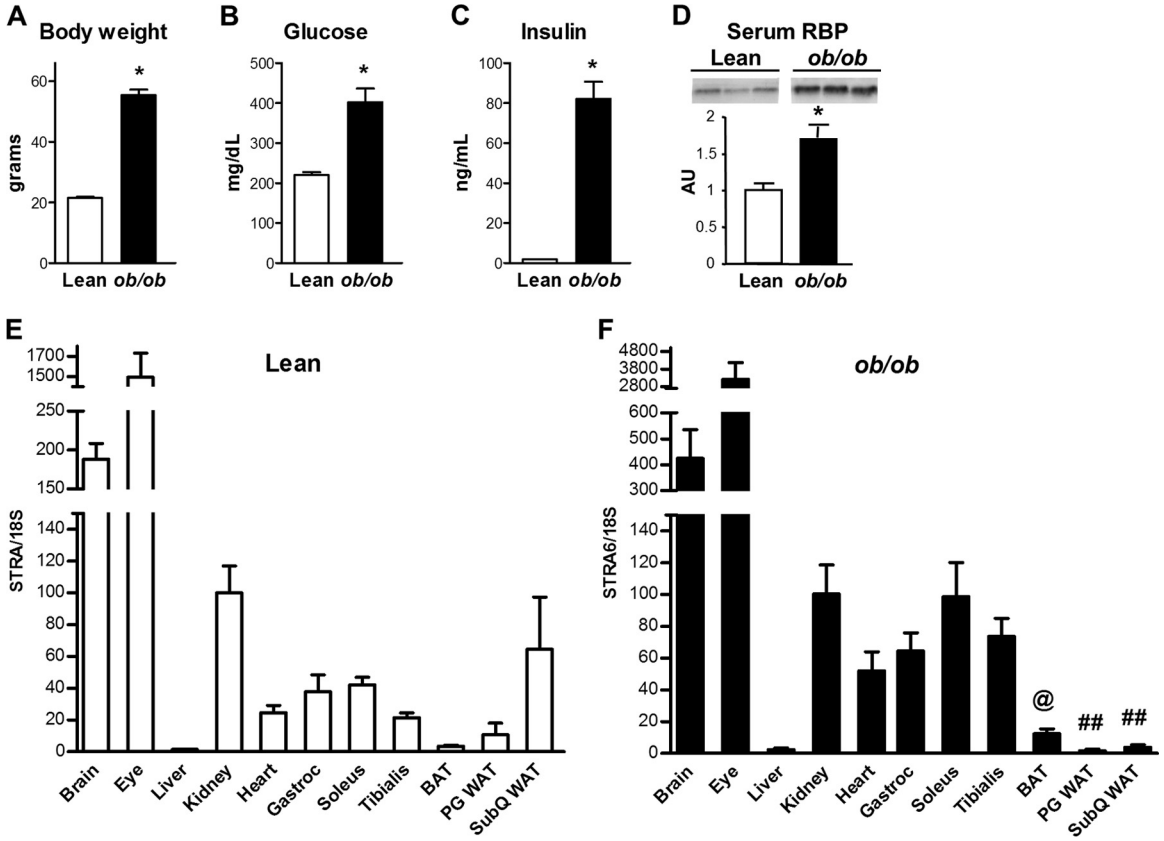

FIG 2 Tissue STRA6 distribution and metabolic characteristics of lean and *ob*/*ob* mice. (A to D) Body weights and fed glucose, fed insulin, and serum RBP4 levels of 3-month-old female lean and *ob*/*ob* mice. *, $P < 0.05$ versus the control. (E) STRA6 mRNA expression in female lean littermates of *ob*/*ob* mice. (F) STRA6 mRNA expression in female *ob*/*ob* mice. All mice were fed a chow diet. @, $P < 0.05$ versus soleus and tibialis muscles; ##, $P < 0.05$ versus all skeletal muscles. All data are expressed relative to levels in kidney in that group of mice and are normalized to 18S rRNA. Analysis performed by ANOVA comparing skeletal muscle, cardiac muscle, and fat depots. Results represent three to five animals per group. Data are expressed as mean ± SEM. Gastroc, gastrocnemius; BAT, brown adipose tissue; PG, perigonadal; WAT, white adipose tissue; SubQ, subcutaneous.

recombined allele was present in adipocytes from adipose-Stra6$^{-/-}$ mice, but it was not present in adipocytes from STRA6 floxed mice or any other tissues from adipose-Stra6$^{-/-}$ mice, including whole brain and kidney tissues (Fig. 5B).

STRA6 mRNA expression was 50 to 65% lower in whole brains and kidneys from both STRA6 flox/flox mice and adipose-Stra6$^{-/-}$ mice than in those from wild-type and adiponectin-Cre controls (Fig. 5C). In contrast, STRA6 expression was not altered in skeletal muscle in STRA6 flox/flox mice and adipose-Stra6$^{-/-}$ mice compared to that in wild-type or adiponectin-Cre controls. Although there was some mouse-to-mouse variation in isolated adipocytes, there was no significant difference in STRA6 expression among the wild-type, adiponectin-Cre, and STRA6 flox/flox groups. STRA6 in perigonadal and subcutaneous adipocytes from adipose-Stra6$^{-/-}$ mice was 50 to 70% lower than in those from wild-type, adiponectin-Cre, and STRA6 flox/flox controls. Thus, although the STRA6 floxed construct itself decreased STRA6 expression in some tissues (whole brain, kidney), STRA6 expression was further reduced specifically in adipocytes from adipose-Stra6$^{-/-}$ mice compared to STRA6 flox/flox mice.

Since no currently available STRA6 antibody detects STRA6 expression in fat (data not shown), we could not measure STRA6 protein levels. Therefore, to determine whether the partial reduction of STRA6 mRNA in some tissues resulted in a systemic phenotype, we extensively characterized the metabolic phenotype of the STRA6 flox/flox mice compared to that of both wild-type and adiponectin-Cre controls. The body weight of STRA6 flox/flox mice fed a chow diet was not different from that of wild-type and adiponectin-Cre controls up to 43 weeks of age (Fig. 6A). Body composition at 8 and 32 weeks (lean mass and fat mass), adipocyte number, and adipocyte size were not different among the genotypes (Fig. 6B to E). There were no differences in serum leptin, glucose tolerance, or insulin sensitivity among wild-type, adiponectin-Cre, and STRA6 flox/flox mice fed a chow diet (Fig. 6F to H). Similarly, when fed a high-fat diet, body weight, serum leptin, fat mass, and lean mass were not different among wild-type, adiponectin-Cre, and STRA6 flox/flox mice (Fig. 6I to L). The partial reduction in STRA6 expression in STRA6 flox/flox mice also did not alter serum RBP4, retinol uptake, and expression of retinoid homeostatic genes in adipocytes (Fig. 6M to P). Therefore, we found no evidence that the partial reduction of STRA6 expression in some tissues had any metabolic effects.

Since STRA6 expression was lower in some tissues containing the STRA6 floxed allele than in wild-type and adiponectin-Cre mice and there were no metabolic changes in the STRA6 flox/flox mice, we used the STRA6 flox/flox mice as controls for all subsequent studies. The reduced STRA6 expression in the brain and kidneys could be due to the effects of the IRES-*lacZ* cassette in the

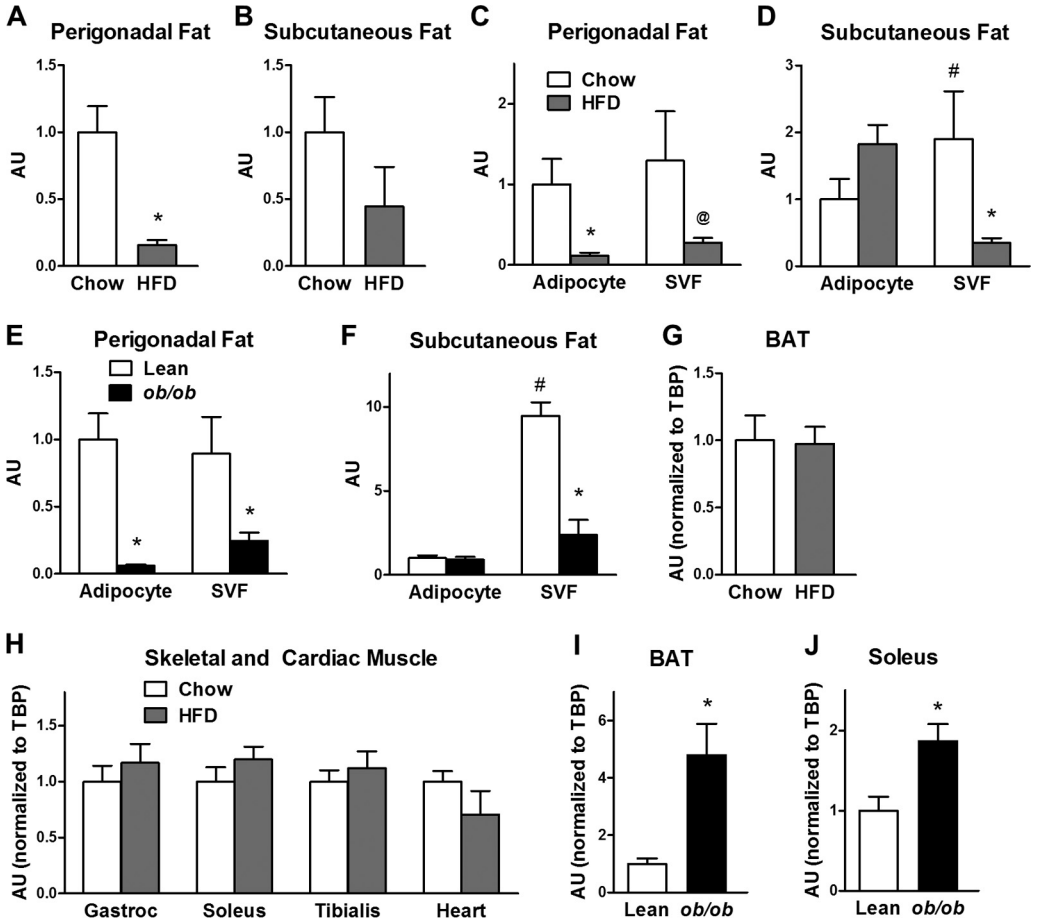

FIG 3 STRA6 expression in whole fat pads, isolated adipocytes, and the SVF in high-fat-diet-fed and *ob*/*ob* mice. (A and B) STRA6 mRNA in whole fat pads in perigonadal fat and subcutaneous fat in chow-fed and high-fat-diet-fed animals. (C and D) STRA6 mRNA in isolated adipocytes and SVF in perigonadal and subcutaneous adipose tissue in mice fed chow or a high-fat diet (HFD). (E and F) STRA6 mRNA in isolated adipocytes and SVF in perigonadal and subcutaneous adipose tissue in lean and *ob*/*ob* mice. For white adipose tissue and adipose tissue fractions, STRA6 expression was calculated by using a standard curve. (G) STRA6/TBP mRNA in brown adipose tissue (BAT) in chow-fed and high-fat-diet-fed mice. (H) STRA6/TBP mRNA in skeletal and cardiac muscles in chow-fed and high-fat-diet-fed mice. Gastroc, gastrocnemius. (I and J) STRA6/TBP mRNA in brown adipose tissue and soleus muscles of lean and *ob*/*ob* mice. *, $P < 0.05$ versus respective control (chow fed or lean); @, $P = 0.07$ versus chow; #, $P < 0.05$ for chow SVF versus chow adipocyte fraction. $n = 4$ to 6 samples per group. For the lean and chow-fed mice, 4 mice were pooled per sample, so the data represent 16 to 24 mice. AU, arbitrary units. Data are expressed as mean ± SEM.

3′ UTR on mRNA stability or to effects on mRNA expression of the *loxP* sites inserted into introns. Several studies in the literature report effects of a floxed construct on the expression of the target gene in specific tissues in the absence of Cre expression (41–43). However, when mice expressing the floxed construct are used as controls, important information can still be obtained.

Characterization of adipose-Stra6$^{-/-}$ mice fed a chow diet. The body weight of adipose-Stra6$^{-/-}$ mice was the same as that of controls at 5 weeks of age, suggesting no congenital growth retardation, and there was a strong trend toward decreased body weight as they got older (Fig. 7A) ($P = 0.06$). At 8 weeks of age, the fat mass and lean mass of adipose-Stra6$^{-/-}$ mice were the same as those of controls, whereas at 32 weeks, adipose-Stra6$^{-/-}$ mice had a 40% decrease in fat mass without altered lean mass (Fig. 7B and C). At 43 weeks, there was a 55% decrease in perigonadal fat weight and a trend toward decreased subcutaneous fat weight in adipose-Stra6$^{-/-}$ mice (Fig. 7D). Adipocyte size was unchanged between genotypes at 17 and 43 weeks of age (Fig. 7E). However, the adipocyte number in perigonadal fat tended to be lower at 17 weeks of age and was lower by 50% at 43 weeks of age, which could account for the leanness in the adipose-Stra6$^{-/-}$ mice (Fig. 7F). Since STRA6 plays a role in adipocyte differentiation (30), we measured the expression of markers of adipocyte differentiation in the adipose-Stra6$^{-/-}$ mice. We found no differences in these markers in adipose tissue between the adipose-Stra6$^{-/-}$ mice and controls (Fig. 7G), suggesting that the decreased cell number was not due to reduced adipocyte differentiation. At 8 weeks of age, serum leptin levels were unchanged in the adipose-Stra6$^{-/-}$ mice (Fig. 7H), consistent with the normal fat mass (Fig. 7B). At 22 weeks of age, leptin levels tended to be lower, and at 33 weeks of age (Fig. 7H), leptin levels were 60% lower in the adipose-Stra6$^{-/-}$ mice, consistent with the lower fat mass (Fig. 7B). Food intake normalized to body weight at 38 weeks did not differ between the adipose-Stra6$^{-/-}$ mice and the controls (Fig. 7I).

To evaluate the mechanism for the decreased adiposity of adipose-Stra6$^{-/-}$ mice, food intake, physical activity, and energy expenditure were measured at 16 weeks of age prior to the divergence in body weight (Fig. 8A). This is the optimal time to detect

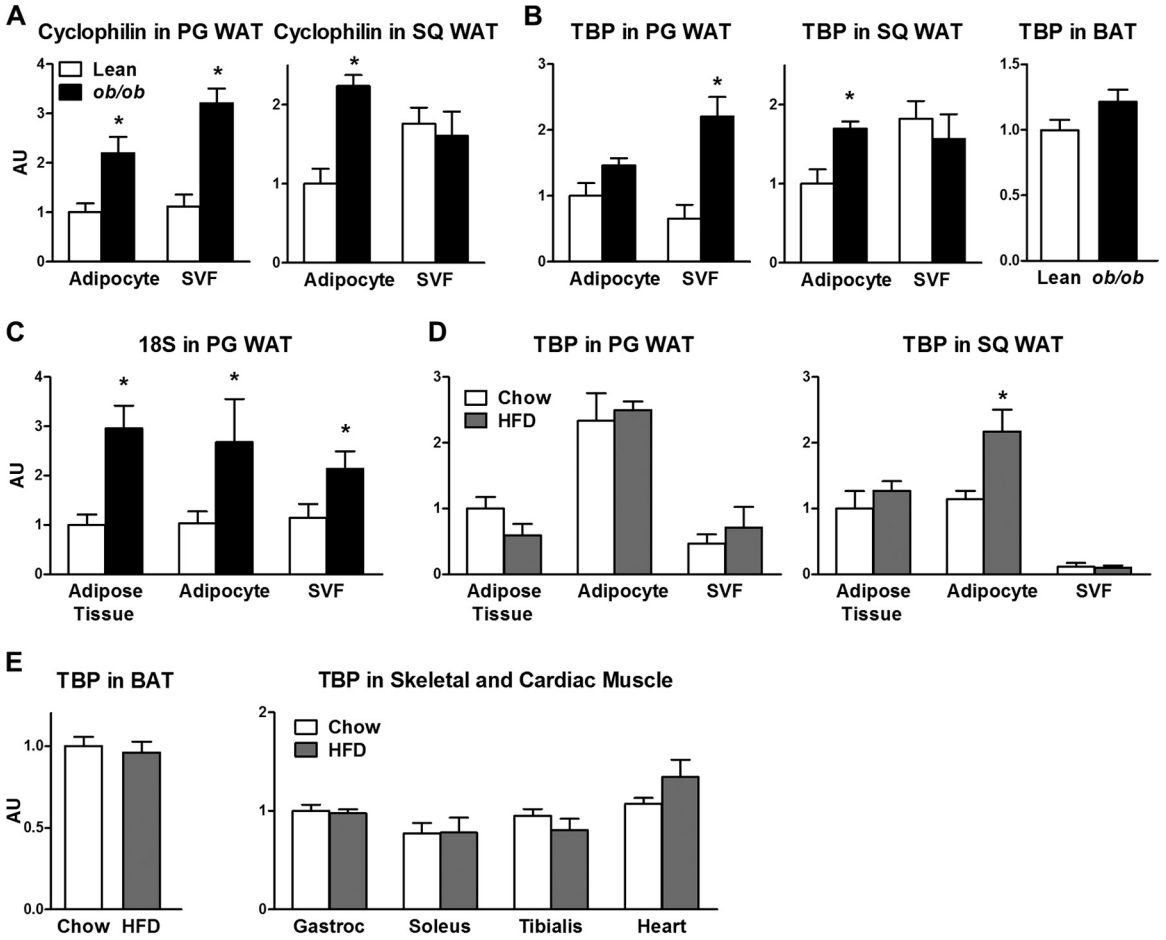

FIG 4 Expression of commonly used housekeeping genes in adipose tissue and muscle. (A) Cyclophilin mRNA in isolated adipocytes and SVF in perigonadal (PG) and subcutaneous (SQ) fat in lean and *ob*/*ob* mice. WAT, white adipose tissue. (B) TBP mRNA in adipocytes and SVF in perigonadal and subcutaneous fat and brown adipose tissue (BAT) of lean and *ob*/*ob* mice. (C) 18S rRNA levels in adipose tissue, isolated adipocytes, and SVF in perigonadal fat of lean and *ob*/*ob* mice. (D) TBP mRNA levels in adipose tissue, adipocytes, and SVF in perigonadal and subcutaneous fat of chow-fed and high-fat-diet (HFD)-fed mice. (E) TBP mRNA levels in brown adipose tissue and muscles of mice fed chow and high-fat diets. $n = 4$ to 6 samples per group. For the lean and chow-fed mice, four mice were pooled per sample, so the data represent 16 to 24 animals. *, $P < 0.05$ versus chow-fed or lean control mice. Data are expressed as mean ± SEM. Gastroc, gastrocnemius.

a difference in energy metabolism, since once a difference in body weight is established, it is more difficult to interpret changes in energy expenditure (44). The mice did not develop decreased adiposity (Fig. 7B and D) because of decreased food intake (Fig. 8B) or increased physical activity (Fig. 8C) ($P = 0.09$), as these parameters were not significantly altered for the adipose-Stra6$^{-/-}$ mice. O_2 consumption, energy expenditure, and CO_2 production during the dark phase showed a very strong trend to increase in adipose-Stra6$^{-/-}$ mice ($P = 0.06$ for these three parameters), which could contribute to the development of leanness (Fig. 8D to F). Resting O_2 consumption (when physical activity is <5% of the baseline) was not significantly altered in adipose-Stra6$^{-/-}$ mice (data not shown). Since altered retinoid metabolism can activate a thermogenic program in adipose tissue (45), we determined if the expression of genes that regulate thermogenic capacity was altered in brown adipose tissue and subcutaneous white adipose tissue in adipose-Stra6$^{-/-}$ mice. Although the expression of classical brown fat markers in brown adipose tissue was not changed (Fig. 8G), there was a striking upregulation of key genes involved in thermogenesis (*Ucp-1*, *Pgc-1a*, and *Cidea*) in the subcutaneous adipose tissue of adipose-Stra6$^{-/-}$ mice (Fig. 8H), consistent with their strong tendency for increased oxygen consumption (Fig. 8E). The expression of other brown selective genes whose biological function is not as well characterized was not altered (Fig. 8H). Browning of white adipose tissue can be mediated by beige adipocytes, which express a unique gene profile (31). The expression of beige selective markers in white adipose tissue was unchanged in adipose-Stra6$^{-/-}$ mice (Fig. 8I).

Serum glucose 5 h after food removal was unchanged in female adipose-Stra6$^{-/-}$ mice fed a chow diet, whereas serum insulin was decreased by ~30 to 40%, indicating increased insulin sensitivity (Fig. 9A and B). The insulin levels were decreased as early as 8 weeks of age, which preceded differences in fat mass and serum leptin, and the decreased insulin persisted at 13 weeks and tended to persist at 22 weeks. In addition, adipose-Stra6$^{-/-}$ mice had improved glucose tolerance, as demonstrated by a decreased area under the curve during GTTs (Fig. 9C), while ITTs (Fig. 9D) were not different, in contrast to the enhanced insulin sensitivity indicated by the reduced ambient insulin levels with normal glucose levels. Data on male adipose-Stra6$^{-/-}$ mice also supported in-

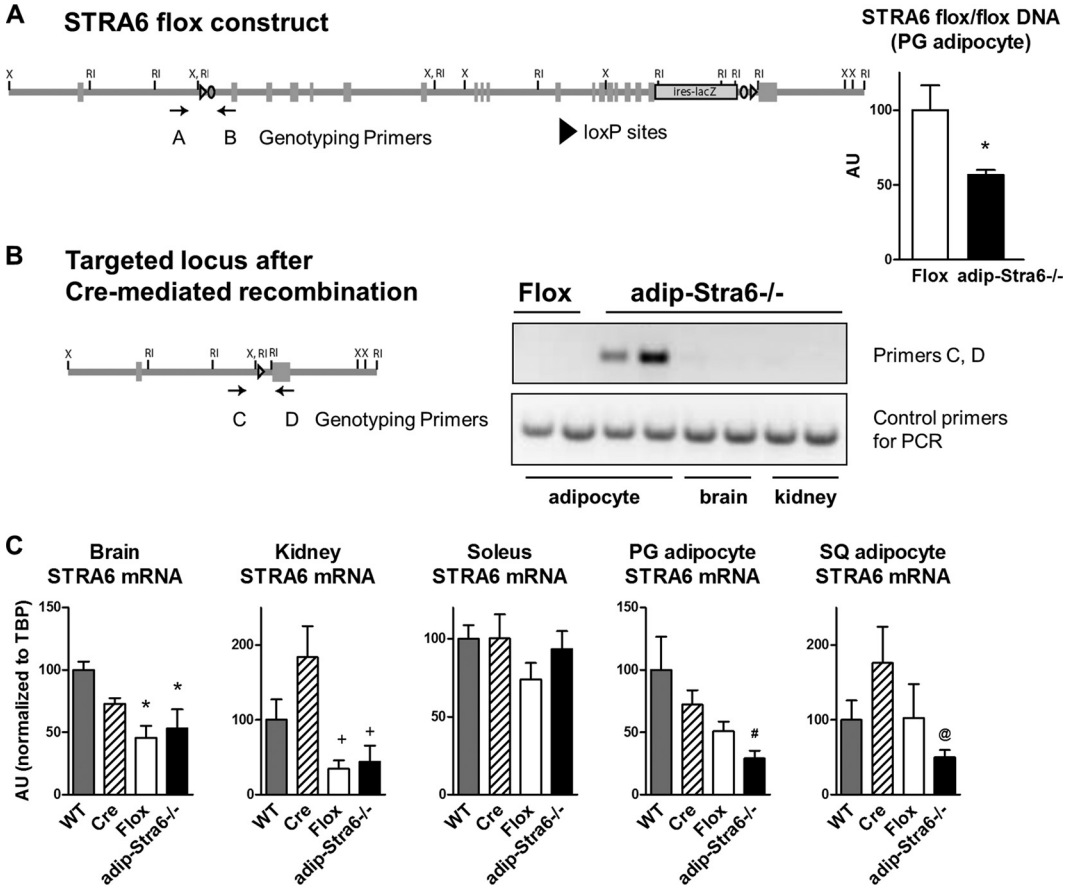

FIG 5 Generation of adipose-Stra6$^{-/-}$ mice. (A) STRA6 flox construct showing *loxP* sites. The STRA6 flox construct contains an IRES-*lacZ* cassette. A PCR assay using DNA from isolated perigonadal adipocytes was done with primers A and B to detect the STRA6 floxed allele. $n = 3$ or 4 per group. *, $P < 0.05$ versus flox. (B) Construct of targeted locus after Cre-mediated recombination. A PCR assay (with primers C and D) was done using DNA from adipocytes from STRA6 flox/flox mice and from adipocytes, kidneys, and whole brains of adipose-Stra6$^{-/-}$ mice. (C) STRA6 mRNA expression in the whole brain, kidney, soleus muscle, perigonadal (PG) adipocytes, and subcutaneous (SQ) adipocytes. $n = 6$ to 12 per group. *, $P < 0.05$ versus the wild type (WT); +, $P < 0.05$ versus adiponectin-Cre (ANOVA comparing all four groups). #, $P < 0.05$ versus all other groups; @, $P < 0.05$ versus the wild type and adiponectin -Cre (*t* test). AU, arbitrary units. Data are expressed as mean ± SEM.

creased insulin sensitivity. Similar to females, male adipose-Stra6$^{-/-}$ mice had normal blood glucose levels, but their insulin levels were lower at 8 weeks of age (1.1 ± 0.1 ng/ml in control mice versus 0.8 ± 0.1 ng/ml in adipose-Stra6$^{-/-}$ mice; $P < 0.05$). This was in spite of normal body weight, perigonadal and subcutaneous fat weight, and serum leptin up to 24 weeks of age (data not shown).

Since STRA6 has been proposed to signal through a JAK2/STAT5 pathway (15) and the STAT5 target gene encoding suppressor of cytokine signaling 3 (SOCS3) modulates insulin sensitivity in adipocytes (46–48), we determined the expression of SOCS3. SOCS3 expression was lower in isolated adipocytes from adipose-Stra6$^{-/-}$ mice than in those from controls (Fig. 9E), which could contribute to the improved insulin sensitivity of these mice. Peroxisome proliferator-activated receptor gamma (PPARγ) has also been proposed as a target of the STRA6/JAK2/STAT5 pathway (15), and PPARγ expression is decreased in white adipose tissue of whole-body STRA6 null mice (18). However, we found no change in PPARγ expression in adipocytes from adipose-Stra6$^{-/-}$ mice (Fig. 9E). To determine the effects of adipose STRA6 knockdown on insulin sensitivity at the cellular level, especially since SOCS3 was decreased, we measured glucose uptake in isolated adipocytes at an age when the perigonadal fat mass was unchanged (Fig. 9F). Basal and insulin-stimulated glucose uptake and the half-maximal effective dose (ED_{50}) were unchanged in isolated adipocytes from adipose-Stra6$^{-/-}$ mice (Fig. 9G).

Characterization of adipose-Stra6$^{-/-}$ mice fed a high-fat diet. We then determined if adipose-Stra6$^{-/-}$ mice were protected from high-fat-diet-induced obesity or insulin resistance. Both control and adipose-Stra6$^{-/-}$ female mice became obese to similar degrees when fed a high-fat diet (Fig. 10A). Body composition studies revealed that fat mass and lean mass were unchanged at 30 weeks of age in the adipose-Stra6$^{-/-}$ mice and the controls (Fig. 10B and C). While the perigonadal fat pad weight in adipose-Stra6$^{-/-}$ mice at 45 weeks of age was lower than that in controls, the subcutaneous fat mass in these mice was unchanged (Fig. 10D). Serum leptin was unchanged at 14 weeks in the adipose-Stra6$^{-/-}$ mice and the controls, consistent with the same degree of adiposity as controls at this age (Fig. 10E). Leptin levels were also the same between genotypes at 45 weeks of age (data not shown). Adipose-Stra6$^{-/-}$ mice had modestly improved insulin sensitiv-

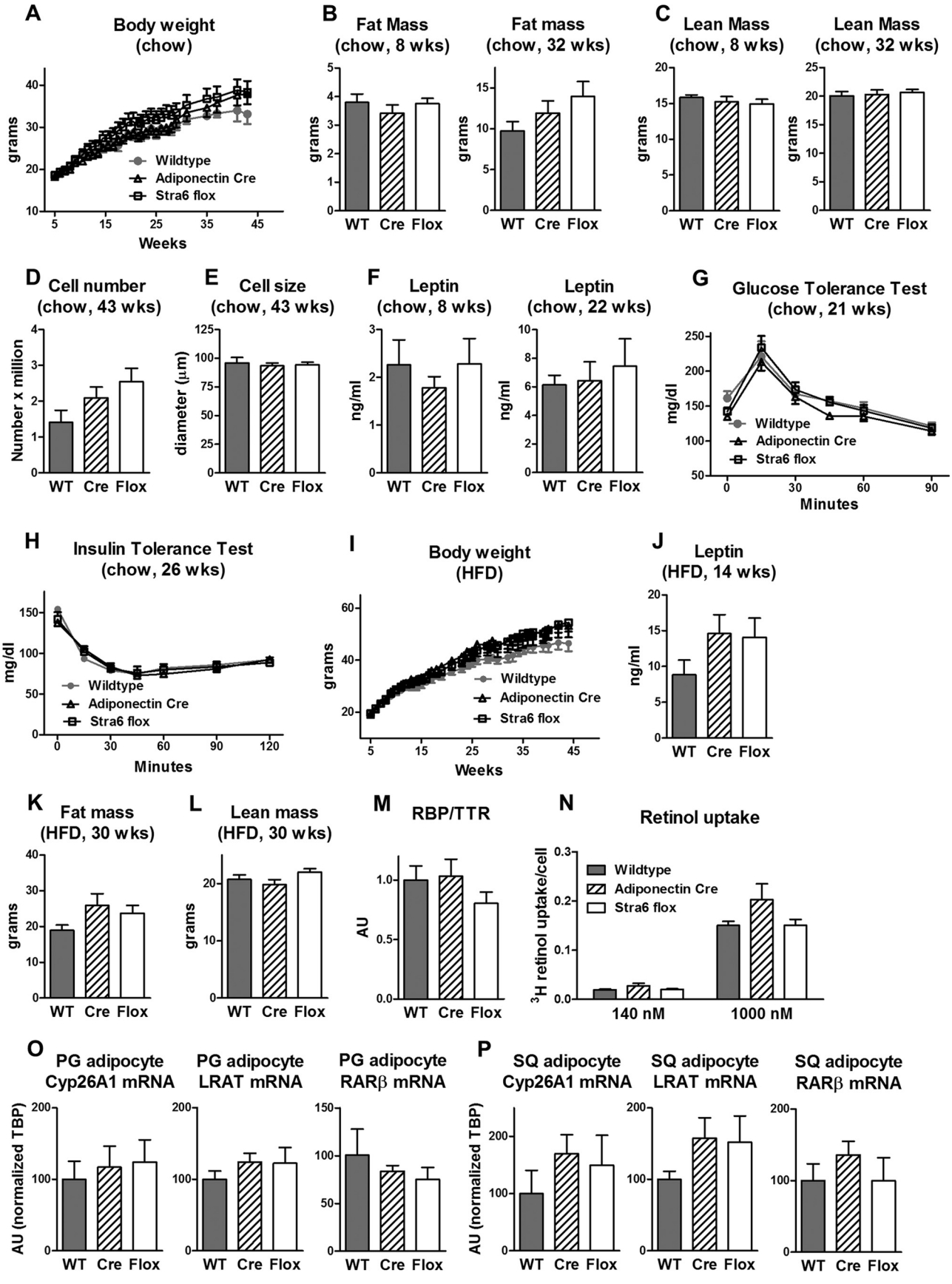
A
Body weight
(chow)
grams
Weeks
Wildtype
Adiponectin Cre
Stra6 flox
B
Fat Mass
(chow, 8 wks)
Fat mass
(chow, 32 wks)
C
Lean Mass
(chow, 8 wks)
Lean Mass
(chow, 32 wks)
WT Cre Flox
D
Cell number
(chow, 43 wks)
Number x million
E
Cell size
(chow, 43 wks)
diameter (μm)
F
Leptin
(chow, 8 wks)
Leptin
(chow, 22 wks)
ng/ml
G
Glucose Tolerance Test
(chow, 21 wks)
mg/dl
Minutes
H
Insulin Tolerance Test
(chow, 26 wks)
I
Body weight
(HFD)
J
Leptin
(HFD, 14 wks)
K
Fat mass
(HFD, 30 wks)
L
Lean mass
(HFD, 30 wks)
M
RBP/TTR
AU
N
Retinol uptake
^{3}H retinol uptake/cell
140 nM
1000 nM
O
PG adipocyte
Cyp26A1 mRNA
PG adipocyte
LRAT mRNA
PG adipocyte
RARβ mRNA
AU (normalized TBP)
P
SQ adipocyte
Cyp26A1 mRNA
SQ adipocyte
LRAT mRNA
SQ adipocyte
RARβ mRNA

ity, as demonstrated by ITT at 16 weeks of age (Fig. 10F), before the divergence of body weight and fat mass.

Overall, the sustained decrease in serum insulin in female adipose-Stra6$^{-/-}$ mice fed a chow diet (Fig. 9B, 8, 13, and 22 weeks old), the decreased serum insulin level in male adipose Stra6$^{-/-}$ mice at 8 weeks of age (1.1 ± 0.1 ng/ml in control mice versus 0.8 ± 0.1 ng/ml in adipose-Stra6$^{-/-}$ mice; $P < 0.05$), and the improved ITT results in female adipose-Stra6$^{-/-}$ mice fed a high-fat diet (Fig. 10F) indicate improved systemic insulin sensitivity in mice with a reduction of STRA6 in adipocytes. The lack of improvement in the ITT results of adipose-Stra6$^{-/-}$ mice on a chow diet suggests that the effects may be relatively mild. The lack of increased insulin sensitivity in the glucose transport assay in isolated adipocytes may indicate that knockdown of adipose STRA6 results in changes in adipose tissue biology that affect insulin action in other tissues or that other pathways in adipocytes, not glucose transport, have increased insulin sensitivity.

Retinoid homeostasis. The serum RBP4/TTR ratio was not altered in adipose-Stra6$^{-/-}$ mice fed a chow diet (Fig. 11A). Retinol uptake with 75 nM [^{3}H]retinol-RBP4 showed a time-dependent increase in isolated perigonadal adipocytes that was not different between control and Stra6$^{-/-}$ adipocytes (Fig. 11B). With higher concentrations of [^{3}H]retinol-RBP4 (140 and 1,000 nM), retinol uptake was also not different between adipocytes from control mice and those from adipose-Stra6$^{-/-}$ mice (Fig. 11C).

Adipose tissue is an important storage site for retinoids, which activate retinoic acid receptor signaling, and the expression of genes involved in retinoid metabolism is a good marker of cellular retinoid levels. The levels of expression of the genes encoding CYP26A1, lecithin retinol acyltransferase (LRAT), and retinoic acid receptor β (RARβ) were not altered in isolated perigonadal (Fig. 11D) or subcutaneous (Fig. 11E) adipocytes from adipose-Stra6$^{-/-}$ mice fed a chow diet or in perigonadal adipose tissue from high-fat-diet-fed mice (data not shown). The expression of these genes was also not altered in the main retinoid storage site, the liver, suggesting no changes in whole-body retinoid homeostasis (data not shown). RBPR2 (or 1300002K09Rik) is a newly described RBP4 receptor and retinol transporter that is highly expressed in the liver with very low expression in adipocytes and the SVF of adipose tissue in chow-fed mice (49). We found very low expression of RBPR2 in the perigonadal adipose tissue of our control mice, and it was not induced in adipose-Stra6$^{-/-}$ mice fed a chow diet (data not shown), indicating that normal retinoid homeostasis did not result from compensatory upregulation of the receptor RBPR2.

DISCUSSION

Since elevated RBP4 causes insulin resistance, we sought to determine the role of its receptor, STRA6, in the pathogenesis of insulin resistance and obesity. Surprisingly, we found that STRA6 was markedly decreased in the adipose tissue but not in the muscle of *ob/ob* mice and mice fed a high-fat diet. Therefore, a key goal of this study was to determine whether knockdown of STRA6 in adipose tissue contributes to insulin resistance or obesity. We achieved a partial knockdown of STRA6 in the adipocytes of adipose-Stra6$^{-/-}$ mice, which should be informative because most therapeutic approaches only partially disrupt receptor-mediated pathways. Our studies provide evidence that mice with a partial reduction in STRA6 in adipocytes have improved insulin sensitivity when fed a chow or high-fat diet. This may be independent of leanness, since in both female and male adipose-Stra6$^{-/-}$ mice fed a chow diet, serum insulin was decreased at an age (8 weeks, Fig. 9B) when body weight and fat mass were unchanged. Furthermore, in high-fat-diet-fed mice, insulin tolerance was improved at 16 weeks (Fig. 10F), when body weight and serum leptin levels (an indication of whole-body fat mass) were unchanged.

We considered several potential mechanisms for the improved insulin sensitivity of adipose-Stra6$^{-/-}$ mice. One possibility is reduced STRA6-dependent action of RBP4, since some studies show that RBP4 may cause insulin resistance in a STRA6-dependent manner (16). Binding of RBP4 to STRA6 has been shown to stimulate JAK2/STAT5 signaling and upregulate STAT target genes, including that for SOCS3 in adipose tissue and muscle (15), and these effects of RBP4 are diminished in whole-body STRA6 null mice (18). We found that isolated adipocytes from adipose-Stra6$^{-/-}$ mice had decreased SOCS3 expression (Fig. 9E), but this was not sufficient to improve insulin-stimulated glucose transport (Fig. 9G). In addition to SOCS3, some data indicate that PPARγ is downstream of STRA6/JAK2/STAT5 signaling (15). PPARγ expression was not decreased in adipocytes from adipose-Stra6$^{-/-}$ mice, in contrast to the decrease in the adipose tissue of whole-body STRA6 null mice (18). The difference could be that in STRA6 null mice, PPARγ expression was measured in adipose tissue in which the macrophages and other stromovascular cells could contribute to the decreased PPARγ expression. Alternatively, total-body knockout of STRA6 may have other effects that indirectly alter PPARγ expression in adipocytes. Another potential mechanism for the improved insulin sensitivity in adipose-Stra6$^{-/-}$ mice could be the increased expression of uncoupling protein 1 (UCP1) in white adipose tissue (Fig. 8H), since even low levels of UCP1 in white adipose tissue improve systemic insulin resistance independently of leanness (50).

We also considered potential mechanisms for leanness in adipose-Stra6$^{-/-}$ mice. The increased expression of UCP1 and other brown selective thermogenic genes in white adipose tissue in these mice likely contributed to their leanness, which, in turn, fostered the sustained improvement in insulin sensitivity. Enhanced brown and beige cell activity is associated with resistance to weight

FIG 6 Adiponectin-Cre and STRA6 flox/flox mice have unchanged body weight, leptin, fat mass, and retinol uptake compared to wild-type mice. (A) Body weights of wild-type, adiponectin-Cre, and STRA6 flox/flox female mice fed a chow diet, which was also used for panels B to H and M to P. $n = 6$ to 12 mice per genotype for chow diet-fed mice. (B and C) Fat mass and lean mass determined by DEXA at 8 and 32 weeks of age. WT, wild type. (D and E) Size and number of adipocytes from perigonadal fat at 43 weeks of age. (F) Serum leptin 5 h after food removal at 8 and 22 weeks of age. (G) GTT (1 g/kg i.p.) of 21-week-old mice. (H) ITT (0.5 U/kg) of 26-week-old mice. (I) Body weights of wild-type, adiponectin-Cre, and STRA6 flox/flox female mice fed a high-fat diet (HFD), which was also used for panels J to L. $n = 5$ to 15 mice per genotype for high-fat-diet-fed mice. (J) Serum leptin levels 5 h after food removal at 14 weeks of age. (K and L) Fat mass and lean mass determined by DEXA at 30 weeks of age. (M) Serum RBP4/TTR levels in mice fed a chow diet at 33 weeks of age. (N) Retinol uptake in isolated perigonadal adipocytes from mice 48 weeks of age. Adipocytes were incubated with 140 or 1,000 nM [^{3}H]retinol-RBP4 for 90 min. Retinol uptake is expressed per adipocyte number. $n = 4$ to 6 per group. (O and P) Levels of CYP26A1, LRAT, and RARβ mRNA expression relative to the TBP expression level in isolated perigonadal (PG) and subcutaneous (SQ) adipocytes. AU, arbitrary units. Data are expressed as mean ± SEM.

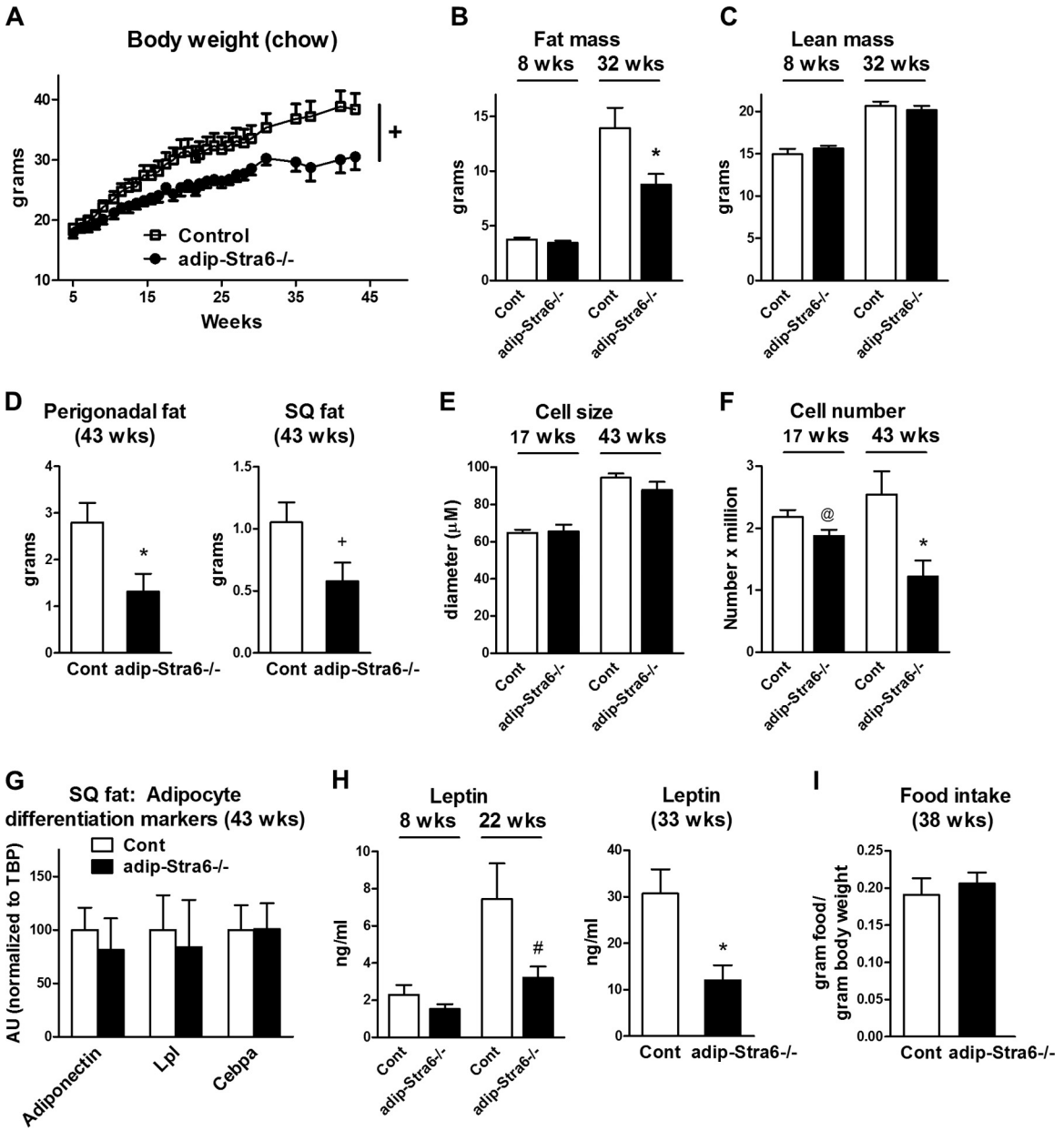

FIG 7 Adipose-Stra6$^{-/-}$ mice have decreased body weight, fat mass, and serum leptin levels when fed a chow diet. (A) Body weights of control and adipose-Stra6$^{-/-}$ mice. +, $P = 0.06$ versus the control (ANOVA). (B and C) Fat mass and lean mass determined by DEXA at 8 and 32 weeks of age. *, $P < 0.05$ versus the control (Cont). (D) Perigonadal and subcutaneous (SQ) fat pad weights at 43 weeks of age. *, $P < 0.05$; +, $P = 0.06$ (versus control mice). (E and F) Size and number of adipocytes from perigonadal fat at 17 and 43 weeks of age. @, $P = 0.07$; *, $P < 0.05$ (versus control mice). (G) Expression of adipocyte differentiation markers in subcutaneous white adipose tissue of mice at 43 weeks of age. AU, arbitrary units. (H) Serum leptin levels 5 h after food removal at 8 and 22 weeks of age: #, $P = 0.08$ versus control mice. Serum leptin levels (mice fed *ad libitum*) at 33 weeks of age: *, $P < 0.05$ versus control mice. (I) Food intake per gram of body weight at 38 weeks of age. All mice were females fed a chow diet. $n = 6$ to 12 per genotype. Data are expressed as mean ± SEM.

gain in several mouse models (51). The leanness could also be due to the decreased adipocyte number (Fig. 7F). One cause for this could be decreased adipocyte differentiation since knockdown of STRA6 in cultured adipocytes was recently shown to impair adipocyte differentiation in the presence of holo-RBP4 (30). However, we did not find differences in white adipocyte differentiation markers, indicating that the reduced adipocyte number did not result from impaired differentiation.

The phenotype of adipose-Stra6$^{-/-}$ mice could be influenced by their genetic background. We found increased insulin sensitivity and decreased fat mass in adipose-Stra6$^{-/-}$ mice on a mixed C57BL/6, 129SvEv, and CD1 background. C57BL/6 mice are more glucose intolerant and hyperinsulinemic than 129 mice fed a chow or high-fat diet (52, 53). In addition, C57BL/6 mice maintained near thermoneutrality have fewer brown adipocytes than Sv129 mice do (54). Therefore, the improvements in insulin sensitivity and leanness observed in adipose-Stra6$^{-/-}$ mice could be strain dependent and more pronounced on a pure C57BL/6 back-

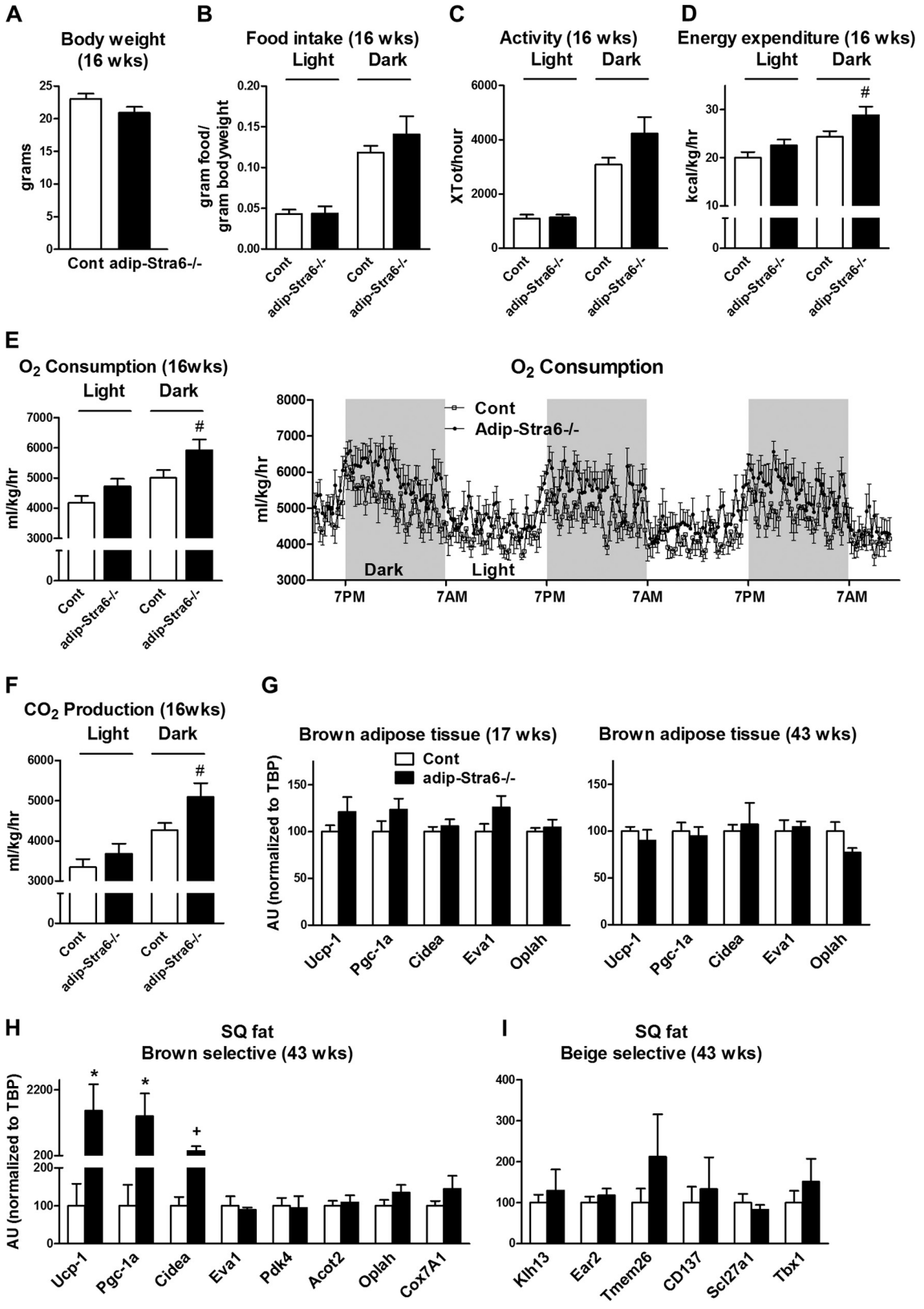

FIG 8 Adipose-Stra6$^{-/-}$ mice show a significant trend toward increased oxygen consumption and increased expression of brown-selective genes in white adipose tissue. (A) Body weights of control (Cont) and adipose-Stra6$^{-/-}$ mice at 16 weeks of age prior to CLAMS studies in panels B to F. (B) Food intake per gram of body weight during the 12-h light and 12-h dark cycle. (C) Activity during the 12-h light and 12-h dark cycle. (D to F) Energy expenditure, O_2 consumption, and CO_2 production during the 12-h light and 12-h dark cycle, which were calculated by using the first full night and day in the CLAMS. (G) mRNA expression of brown-selective genes in brown adipose tissue at 17 and 43 weeks of age. (H) Brown-selective marker expression in subcutaneous (SQ) white adipose tissue in mice at 43 weeks of age. (I) Expression of beige-selective markers in subcutaneous white adipose tissue in mice at 43 weeks of age. $n = 7$ or 8 per genotype for CLAMS; $n = 4$ to 6 per group for gene expression at 43 weeks of age. *, $P < 0.05$; #, $P = 0.06$; +, $P = 0.07$ (versus control mice). All mice were females fed a chow diet. AU, arbitrary units. Data are expressed as mean ± SEM.

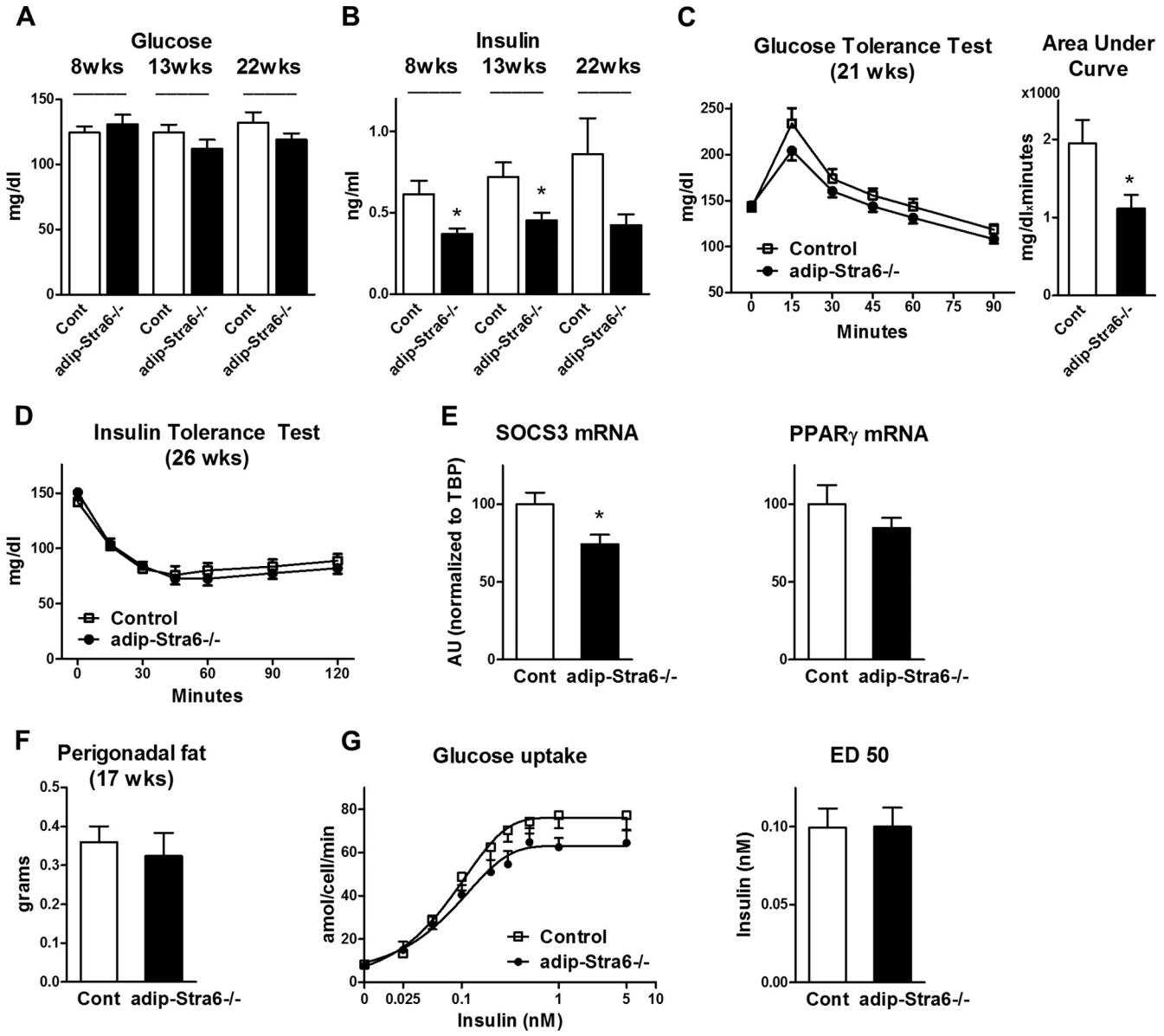

FIG 9 Adipose-Stra6$^{-/-}$ mice have decreased serum insulin levels and improved glucose tolerance when fed a chow diet. (A and B) Serum glucose and insulin levels in 8-, 13-, and 22-week-old female mice 5 h after food removal. *, $P < 0.05$ versus control mice (Cont). (C) GTT (1 g/kg i.p.) and area under the curve (0 to 45 min) of 21-week-old mice. *, $P < 0.05$ versus control mice. (D) ITT (0.5 U/kg) of 26-week-old mice. (E) SOCS3 mRNA and PPARγ mRNA levels in isolated perigonadal adipocytes. *, $P < 0.05$ versus control mice. (F) Perigonadal fat weight in mice at 17 weeks of age prior to the glucose uptake study. (G) Glucose uptake expressed per adipocyte at the indicated insulin concentrations and ED_{50} in isolated perigonadal adipocytes. All mice were females fed a chow diet. n = 6 to 12 mice per genotype. AU, arbitrary units. Data are expressed as mean ± SEM.

ground. We also observed gender differences in the leanness phenotype of adipose-Stra6$^{-/-}$ mice, although both genders had increased insulin sensitivity. Female adipose-Stra6$^{-/-}$ mice had lower body weights as they got older, whereas male adipose-Stra6$^{-/-}$ mice had normal body weights and serum leptin levels up to 24 weeks of age, although leanness in males could emerge at a later age. Sexual dimorphisms have been observed in several mouse models of obesity (55) and diabetes (56, 57). Vitamin A metabolism may be important in these sexual dimorphisms, since female mice, but not male mice, with a block in vitamin A metabolism are resistant to the high-fat-diet-induced formation of visceral fat (58).

Another major finding of this study was a marked decrease in STRA6 expression in adipose tissue in high-fat-diet-fed wild-type mice and *ob*/*ob* mice. This could be surprising since signaling through STRA6 has been proposed to cause insulin resistance (15, 59). We considered potential mechanisms for the decrease in STRA6 expression. STRA6 has been shown to be induced by retinoic acid (10–12), Wnt-1 (12), and p53 (60). However, these mechanisms do not appear to explain the marked decrease in STRA6 in adipose tissue of high-fat-diet-fed mice or *ob*/*ob* mice since retinoic acid levels and retinoic acid receptor signaling are not reduced in adipose tissue in these models (61; data not shown). Furthermore, p53 is increased in *ob*/*ob* mouse adipose

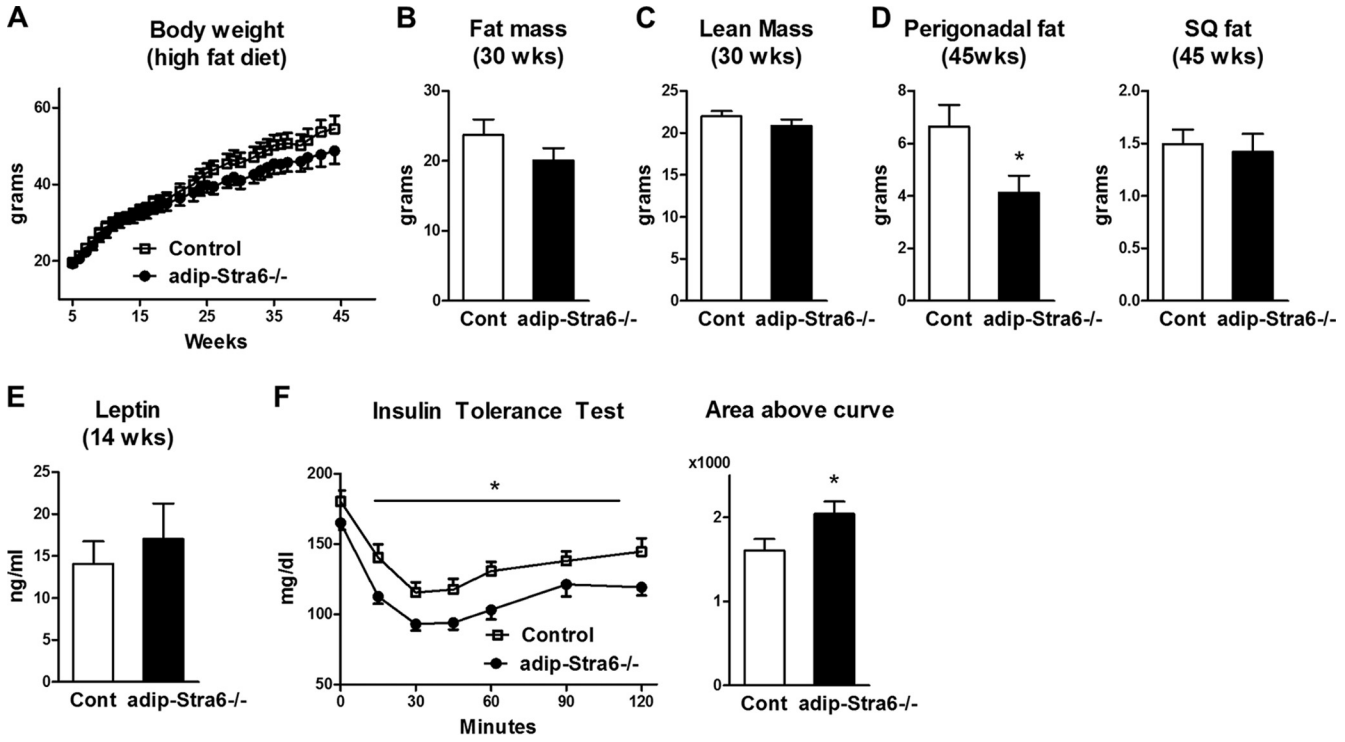

FIG 10 Adipose-Stra6$^{-/-}$ mice have improved insulin tolerance when fed a high-fat diet. (A) Body weights of control (Cont) and adipose-Stra6$^{-/-}$ mice. (B and C) Fat mass and lean mass determined by DEXA at 30 weeks of age. (D) Perigonadal and subcutaneous (SQ) fat pad weights at 45 weeks of age. (E) Serum leptin 5 h after food removal at 14 weeks of age. (F) ITT (0.7 U/kg) in 16-week-old mice. Area above the curve during an ITT from 0 to 60 min, which was calculated by using values relative to the starting glucose level. *, $P < 0.05$ versus control mice. All mice were females fed a high-fat diet. $n = 5$ to 15 mice per genotype. Data are expressed as mean ± SEM.

tissue (62), and Wnt-1 is normally restricted to the testes in adult mice (63, 64). In future studies, it would be of interest to determine if other Wnt proteins regulate STRA6 expression in adipose tissue.

The downregulation of STRA6 in adipose tissue indicates that STRA6 may not contribute significantly to insulin resistance in high-fat-diet-induced and *ob*/*ob* models of obesity. Both of these models have a 1.5- to 4-fold increase in serum RBP4 (65), which is similar to the elevation in obese, insulin-resistant humans (2, 3). Elevated serum RBP4 contributes to insulin resistance, since lowering it improves insulin sensitivity in mice (4, 66, 67). The marked decrease in STRA6 (Fig. 1 to 3) indicates that the insulin resistance may result from STRA6-independent mechanisms of RBP4 action. Recent data demonstrate that RBP4 causes insulin resistance by inducing the immune system independently of STRA6 (68). Immune system activation is thought to be an important cause of obesity-induced insulin resistance (69). A 2- to 3-fold elevation of serum RBP4 appears to be sufficient to activate the immune system in adipose tissue, since RBP4-overexpressing transgenic mice with this level of serum RBP4 have insulin resistance in the absence of obesity. This appears to result from RBP4-induced macrophage infiltration and proinflammatory cytokine production in adipose tissue (68). RBP4 activates macrophages directly, even though these cells do not express STRA6 and these effects are mediated by Toll-like receptor 4 (14, 70). This indicates that modest increases in RBP4 can cause inflammation in adipose tissue in a STRA6-independent manner. Similar effects are seen in cultured endothelial cells which also do not express STRA6 (13).

Since STRA6 has been implicated in cellular retinol uptake, we determined the roles of STRA6 in adipocytes in retinol uptake and in retinoid homeostasis. Retinol uptake was not altered in isolated adipocytes with a partial reduction in STRA6 (Fig. 11B), indicating that full STRA6 levels are not required for normal retinol uptake. Consistent with these findings, mice in which STRA6 is more completely knocked out have a less than ~25% decrease in retinol uptake into white adipose tissue *in vivo* (18, 59). In our studies, the lack of effect on retinol uptake does not appear to be due to compensation of RBPR2 since we did not find compensatory upregulation in adipose tissue of adipose-Stra6$^{-/-}$ mice. Since retinol uptake via STRA6 is coupled to LRAT (71, 72), which is regulated by retinoids (73), one might expect LRAT expression to be altered in adipocytes of adipose-Stra6$^{-/-}$ mice. However, the expression of neither the gene for LRAT nor other retinoid homeostatic genes (encoding CYP26A1 and RARβ) was changed in adipocytes from these mice, which suggests normal tissue retinoid levels.

In summary, the reduction of STRA6 in adipocytes results in leanness and improved insulin sensitivity, which may be due to the increased expression of brown selective genes in white adipose tissue. These findings and genetic studies that show that STRA6 polymorphisms are associated with type 2 diabetes (17) indicate that STRA6 in adipocytes may be important in the maintenance of normal body fat and physiological insulin action. It has been hypothesized that increased signaling through STRA6 could cause insulin resistance (15), but this does not appear to be the case in high-fat fed and *ob*/*ob* models of obesity, since STRA6 expression was markedly downregulated in adipose tissue in these models.

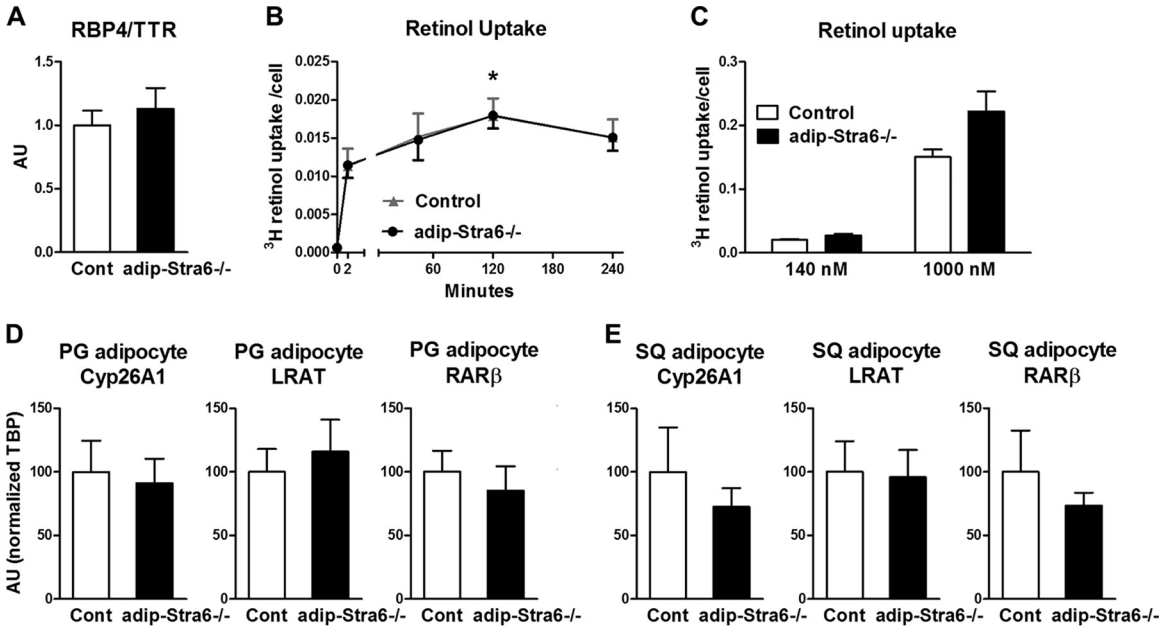

FIG 11 Adipocytes from adipose-Stra6$^{-/-}$ mice demonstrate unchanged retinol uptake and expression of retinoid homeostatic genes. (A) Serum RBP4/TTR levels in mice fed a chow diet at 33 weeks of age. Cont, control. (B) Retinol uptake in isolated perigonadal adipocytes from 48-week-old female adipose-Stra6$^{-/-}$ mice treated with 75 nM [^{3}H]retinol-RBP4 for the durations indicated. $n = 4$ for each time point and condition. *, $P < 0.05$ versus 2-min time point. (C) Retinol uptake in isolated perigonadal adipocytes from 48-week-old female adipose-Stra6$^{-/-}$ mice. Adipocytes were incubated with 140 or 1,000 nM [^{3}H]retinol-RBP4 for 90 min. Retinol uptake is expressed per adipocyte number. $n = 4$ to 6 per group. (D and E) Levels of CYP26A1, LRAT, and RARβ mRNA expression relative to the TBP expression levels in isolated perigonadal (PG) and subcutaneous (SQ) adipocytes. AU, arbitrary units. Data are expressed as mean ± SEM.

This is consistent with prior studies that indicate that RBP4 causes insulin resistance and inflammation in a STRA6-independent manner (13, 14, 68). The determination of the biological effects of other cell surface receptors that are activated by RBP4 may lead to a greater understanding of the mechanisms of RBP4-induced insulin resistance in the pathogenesis of type 2 diabetes and metabolic syndrome.

ACKNOWLEDGMENTS

This work was supported by National Institutes of Health grants NIDDK K08 DK084344 (to L.Z.), NIDDK F32 DK091041 (to J.N.), and NIDDK R37 DK43051 and P30 DK57521 (to B.B.K). B.J.K. was supported by a research fellowship from the German Cardiac Society (Bayer-Forschungsstipendium). CLAMS studies were performed at the Harvard Neuro-Discovery Center, which subsidized a portion of the behavioral study.

We thank N. B. Ghyselinck for reagents and W. S. Blaner for helpful advice.

REFERENCES

1. **Danaei G, Finucane MM, Lin JK, Singh GM, Paciorek CJ, Cowan MJ, Farzadfar F, Stevens GA, Lim SS, Riley LM, Ezzati M.** 2011. National, regional, and global trends in systolic blood pressure since 1980: systematic analysis of health examination surveys and epidemiological studies with 786 country-years and 5.4 million participants. Lancet **377:**568–577. http://dx.doi.org/10.1016/S0140-6736(10)62036-3.
2. **Graham TE, Yang Q, Bluher M, Hammarstedt A, Ciaraldi TP, Henry RR, Wason CJ, Oberbach A, Jansson PA, Smith U, Kahn BB.** 2006. Retinol-binding protein 4 and insulin resistance in lean, obese, and diabetic subjects. N. Engl. J. Med. **354:**2552–2563. http://dx.doi.org/10.1056/NEJMoa054862.
3. **Klöting N, Graham TE, Berndt J, Kralisch S, Kovacs P, Wason CJ, Fasshauer M, Schon MR, Stumvoll M, Bluher M, Kahn BB.** 2007. Serum retinol-binding protein is more highly expressed in visceral than in subcutaneous adipose tissue and is a marker of intra-abdominal fat mass. Cell Metab. **6:**79–87. http://dx.doi.org/10.1016/j.cmet.2007.06.002.
4. **Yang Q, Graham TE, Mody N, Preitner F, Peroni OD, Zabolotny JM, Kotani K, Quadro L, Kahn BB.** 2005. Serum retinol binding protein 4 contributes to insulin resistance in obesity and type 2 diabetes. Nature **436:**356–362. http://dx.doi.org/10.1038/nature03711.
5. **van Hoek M, Dehghan A, Zillikens MC, Hofman A, Witteman JC, Sijbrands EJ.** 2008. An RBP4 promoter polymorphism increases risk of type 2 diabetes. Diabetologia **51:**1423–1428. http://dx.doi.org/10.1007/s00125-008-1042-8.
6. **Meisinger C, Ruckert IM, Rathmann W, Doring A, Thorand B, Huth C, Kowall B, Koenig W.** 2011. Retinol-binding protein 4 is associated with prediabetes in adults from the general population: the Cooperative Health Research in the Region of Augsburg (KORA) F4 Study. Diabetes Care **34:**1648–1650. http://dx.doi.org/10.2337/dc11-0118.
7. **Kaess BM, Enserro DM, McManus DD, Xanthakis V, Chen MH, Sullivan LM, Ingram C, O'Donnell CJ, Keaney JF, Vasan RS, Glazer NL.** 2012. Cardiometabolic correlates and heritability of fetuin-A, retinol-binding protein 4, and fatty-acid binding protein 4 in the Framingham Heart Study. J. Clin. Endocrinol. Metab. **97:**E1943–1947. http://dx.doi.org/10.1210/jc.2012-1458.
8. **Qi Q, Yu Z, Ye X, Zhao F, Huang P, Hu FB, Franco OH, Wang J, Li H, Liu Y, Lin X.** 2007. Elevated retinol-binding protein 4 levels are associated with metabolic syndrome in Chinese people. J. Clin. Endocrinol. Metab. **92:**4827–4834. http://dx.doi.org/10.1210/jc.2007-1219.
9. **Sun Q, Kiernan UA, Shi L, Phillips DA, Kahn BB, Hu FB, Manson JE, Albert CM, Rexrode KM.** 2013. Plasma retinol-binding protein 4 (RBP4) levels and risk of coronary heart disease: a prospective analysis among women in the nurses' health study. Circulation **127:**1938–1947. http://dx.doi.org/10.1161/CIRCULATIONAHA.113.002073.
10. **Kawaguchi R, Yu J, Honda J, Hu J, Whitelegge J, Ping P, Wiita P, Bok D, Sun H.** 2007. A membrane receptor for retinol binding protein mediates cellular uptake of vitamin A. Science **315:**820–825. http://dx.doi.org/10.1126/science.1136244.
11. **Bouillet P, Sapin V, Chazaud C, Messaddeq N, Decimo D, Dolle P, Chambon P.** 1997. Developmental expression pattern of Stra6, a retinoic acid-responsive gene encoding a new type of membrane protein. Mech. Dev. **63:**173–186. http://dx.doi.org/10.1016/S0925-4773(97)00039-7.
12. **Szeto W, Jiang W, Tice DA, Rubinfeld B, Hollingshead PG, Fong SE, Dugger DL, Pham T, Yansura DG, Wong TA, Grimaldi JC, Corpuz RT,**

Singh JS, Frantz GD, Devaux B, Crowley CW, Schwall RH, Eberhard DA, Rastelli L, Polakis P, Pennica D. 2001. Overexpression of the retinoic acid-responsive gene Stra6 in human cancers and its synergistic induction by Wnt-1 and retinoic acid. Cancer Res. **61:**4197–4205. http://cancerres.aacrjournals.org/cgi/pmidlookup?view=long&pmid=11358845.

13. **Farjo KM, Farjo RA, Halsey S, Moiseyev G, Ma JX.** 2012. Retinol-binding protein 4 induces inflammation in human endothelial cells by an NADPH oxidase- and nuclear factor kappa B-dependent and retinol-independent mechanism. Mol. Cell. Biol. **32:**5103–5115. http://dx.doi.org/10.1128/MCB.00820-12.
14. **Norseen J, Hosooka T, Hammarstedt A, Yore MM, Kant S, Aryal P, Kiernan UA, Phillips DA, Maruyama H, Kraus BJ, Usheva A, Davis RJ, Smith U, Kahn BB.** 2012. Retinol-binding protein 4 inhibits insulin signaling in adipocytes by inducing proinflammatory cytokines in macrophages through a c-Jun N-terminal kinase- and Toll-like receptor 4-dependent and retinol-independent mechanism. Mol. Cell. Biol. **32:**2010–2019. http://dx.doi.org/10.1128/MCB.06193-11.
15. **Berry DC, Jin H, Majumdar A, Noy N.** 2011. Signaling by vitamin A and retinol-binding protein regulates gene expression to inhibit insulin responses. Proc. Natl. Acad. Sci. U. S. A. **108:**4340–4345. http://dx.doi.org/10.1073/pnas.1011115108.
16. **Chen CH, Hsieh TJ, Lin KD, Lin HY, Lee MY, Hung WW, Hsiao PJ, Shin SJ.** 2012. Increased unbound retinol-binding protein 4 concentration induces apoptosis through receptor-mediated signaling. J. Biol. Chem. **287:**9694–9707. http://dx.doi.org/10.1074/jbc.M111.301721.
17. **Nair AK, Sugunan D, Kumar H, Anilkumar G.** 2010. Case-control analysis of SNPs in GLUT4, RBP4 and STRA6: association of SNPs in STRA6 with type 2 diabetes in a South Indian population. PLoS One **5:**e11444. http://dx.doi.org/10.1371/journal.pone.0011444.
18. **Berry DC, Jacobs H, Marwarha G, Gely-Pernot A, O'Byrne SM, DeSantis D, Klopfenstein M, Feret B, Dennefeld C, Blaner WS, Croniger CM, Mark M, Noy N, Ghyselinck NB.** 2013. The STRA6 receptor is essential for retinol-binding protein-induced insulin resistance but not for maintaining vitamin A homeostasis in tissues other than the eye. J. Biol. Chem. **288:**24528–24539. http://dx.doi.org/10.1074/jbc.M113.484014.
19. **Golzio C, Martinovic-Bouriel J, Thomas S, Mougou-Zrelli S, Grattagliano-Bessieres B, Bonniere M, Delahaye S, Munnich A, Encha-Razavi F, Lyonnet S, Vekemans M, Attie-Bitach T, Etchevers HC.** 2007. Matthew-Wood syndrome is caused by truncating mutations in the retinol-binding protein receptor gene STRA6. Am. J. Hum. Genet. **80:**1179–1187. http://dx.doi.org/10.1086/518177.
20. **Pasutto F, Sticht H, Hammersen G, Gillessen-Kaesbach G, Fitzpatrick DR, Nurnberg G, Brasch F, Schirmer-Zimmermann H, Tolmie JL, Chitayat D, Houge G, Fernandez-Martinez L, Keating S, Mortier G, Hennekam RC, von der Wense A, Slavotinek A, Meinecke P, Bitoun P, Becker C, Nurnberg P, Reis A, Rauch A.** 2007. Mutations in STRA6 cause a broad spectrum of malformations including anophthalmia, congenital heart defects, diaphragmatic hernia, alveolar capillary dysplasia, lung hypoplasia, and mental retardation. Am. J. Hum. Genet. **80:**550–560. http://dx.doi.org/10.1086/512203.
21. **West B, Bove KE, Slavotinek AM.** 2009. Two novel STRA6 mutations in a patient with anophthalmia and diaphragmatic eventration. Am. J. Med. Genet. A **149A:**539–542. http://dx.doi.org/10.1002/ajmg.a.32682.
22. **White T, Lu T, Metlapally R, Katowitz J, Kherani F, Wang TY, Tran-Viet KN, Young TL.** 2008. Identification of STRA6 and SKI sequence variants in patients with anophthalmia/microphthalmia. Mol. Vis. **14:**2458–2465. http://www.ncbi.nlm.nih.gov/pmc/articles/PMC2610290/.
23. **Ruiz A, Mark M, Jacobs H, Klopfenstein M, Hu J, Lloyd M, Habib S, Tosha C, Radu RA, Ghyselinck NB, Nusinowitz S, Bok D.** 2012. Retinoid content, visual responses, and ocular morphology are compromised in the retinas of mice lacking the retinol-binding protein receptor, STRA6. Invest. Ophthalmol. Vis. Sci. **53:**3027–3039. http://dx.doi.org/10.1167/iovs.11-8476.
24. **Tsutsumi C, Okuno M, Tannous L, Piantedosi R, Allan M, Goodman DS, Blaner WS.** 1992. Retinoids and retinoid-binding protein expression in rat adipocytes. J. Biol. Chem. **267:**1805–1810.
25. **Kurlandsky SB, Gamble MV, Ramakrishnan R, Blaner WS.** 1995. Plasma delivery of retinoic acid to tissues in the rat. J. Biol. Chem. **270:**17850–17857. http://dx.doi.org/10.1074/jbc.270.30.17850.
26. **D'Ambrosio DN, Clugston RD, Blaner WS.** 2011. Vitamin A metabolism: an update. Nutrients **3:**63–103. http://dx.doi.org/10.3390/nu3010063.
27. **Galic S, Oakhill JS, Steinberg GR.** 2010. Adipose tissue as an endocrine organ. Mol. Cell. Endocrinol. **316:**129–139. http://dx.doi.org/10.1016/j.mce.2009.08.018.
28. **Lee KY, Russell SJ, Ussar S, Boucher J, Vernochet C, Mori MA, Smyth G, Rourk M, Cederquist C, Rosen ED, Kahn BB, Kahn CR.** 2013. Lessons on conditional gene targeting in mouse adipose tissue. Diabetes **62:**864–874. http://dx.doi.org/10.2337/db12-1089.
29. **Eguchi J, Wang X, Yu S, Kershaw EE, Chiu PC, Dushay J, Estall JL, Klein U, Maratos-Flier E, Rosen ED.** 2011. Transcriptional control of adipose lipid handling by IRF4. Cell Metab. **13:**249–259. http://dx.doi.org/10.1016/j.cmet.2011.02.005.
30. **Muenzner M, Tuvia N, Deutschmann C, Witte N, Tolkachov A, Valai A, Henze A, Sander LE, Raila J, Schupp M.** 2013. RBP4 and its membrane receptor STRA6 control adipogenesis by regulating cellular retinoid homeostasis and RARalpha activity. Mol. Cell. Biol. **33:**4068–4082. http://dx.doi.org/10.1128/MCB.00221-13.
31. **Wu J, Bostrom P, Sparks LM, Ye L, Choi JH, Giang AH, Khandekar M, Virtanen KA, Nuutila P, Schaart G, Huang K, Tu H, van Marken Lichtenbelt WD, Hoeks J, Enerback S, Schrauwen P, Spiegelman BM.** 2012. Beige adipocytes are a distinct type of thermogenic fat cell in mouse and human. Cell **150:**366–376. http://dx.doi.org/10.1016/j.cell.2012.05.016.
32. **Xu Z, Yu S, Hsu CH, Eguchi J, Rosen ED.** 2008. The orphan nuclear receptor chicken ovalbumin upstream promoter-transcription factor II is a critical regulator of adipogenesis. Proc. Natl. Acad. Sci. U. S. A. **105:**2421–2426. http://dx.doi.org/10.1073/pnas.0707082105.
33. **Shepherd PR, Gnudi L, Tozzo E, Yang H, Leach F, Kahn BB.** 1993. Adipose cell hyperplasia and enhanced glucose disposal in transgenic mice overexpressing GLUT4 selectively in adipose tissue. J. Biol. Chem. **268:**22243–22246.
34. **Cushman SW, Salans LB.** 1978. Determinations of adipose cell size and number in suspensions of isolated rat and human adipose cells. J. Lipid Res. **19:**269–273.
35. **Tozzo E, Gnudi L, Kahn BB.** 1997. Amelioration of insulin resistance in streptozotocin diabetic mice by transgenic overexpression of GLUT4 driven by an adipose-specific promoter. Endocrinology **138:**1604–1611. http://dx.doi.org/10.1210/endo.138.4.5043.
36. **Jensen MD.** 2008. Role of body fat distribution and the metabolic complications of obesity. J. Clin. Endocrinol. Metab. **93:**S57–S63. http://dx.doi.org/10.1210/jc.2008-1585.
37. **Timmons JA, Wennmalm K, Larsson O, Walden TB, Lassmann T, Petrovic N, Hamilton DL, Gimeno RE, Wahlestedt C, Baar K, Nedergaard J, Cannon B.** 2007. Myogenic gene expression signature establishes that brown and white adipocytes originate from distinct cell lineages. Proc. Natl. Acad. Sci. U. S. A. **104:**4401–4406. http://dx.doi.org/10.1073/pnas.0610615104.
38. **Seale P, Bjork B, Yang W, Kajimura S, Chin S, Kuang S, Scime A, Devarakonda S, Conroe HM, Erdjument-Bromage H, Tempst P, Rudnicki MA, Beier DR, Spiegelman BM.** 2008. PRDM16 controls a brown fat/skeletal muscle switch. Nature **454:**961–967. http://dx.doi.org/10.1038/nature07182.
39. **Dugail I, Quignard-Boulange A, Bazin R, Le Liepvre X, Lavau M.** 1988. Adipose-tissue-specific increase in glyceraldehyde-3-phosphate dehydrogenase activity and mRNA amounts in suckling pre-obese Zucker rats. Effect of weaning. Biochem. J. **254:**483–487.
40. **Catalán V, Gomez-Ambrosi J, Rotellar F, Silva C, Rodriguez A, Salvador J, Gil MJ, Cienfuegos JA, Fruhbeck G.** 2007. Validation of endogenous control genes in human adipose tissue: relevance to obesity and obesity-associated type 2 diabetes mellitus. Horm. Metab. Res. **39:**495–500. http://dx.doi.org/10.1055/s-2007-982502.
41. **Abel ED, Kaulbach HC, Tian R, Hopkins JC, Duffy J, Doetschman T, Minnemann T, Boers ME, Hadro E, Oberste-Berghaus C, Quist W, Lowell BB, Ingwall JS, Kahn BB.** 1999. Cardiac hypertrophy with preserved contractile function after selective deletion of GLUT4 from the heart. J. Clin. Invest. **104:**1703–1714. http://dx.doi.org/10.1172/JCI7605.
42. **Sakamoto K, McCarthy A, Smith D, Green KA, Grahame Hardie D, Ashworth A, Alessi DR.** 2005. Deficiency of LKB1 in skeletal muscle prevents AMPK activation and glucose uptake during contraction. EMBO J. **24:**1810–1820. http://dx.doi.org/10.1038/sj.emboj.7600667.
43. **Postic C, Shiota M, Niswender KD, Jetton TL, Chen Y, Moates JM, Shelton KD, Lindner J, Cherrington AD, Magnuson MA.** 1999. Dual roles for glucokinase in glucose homeostasis as determined by liver and pancreatic beta cell-specific gene knock-outs using Cre recombinase. J. Biol. Chem. **274:**305–315. http://dx.doi.org/10.1074/jbc.274.1.305.

44. **Tschöp MH, Speakman JR, Arch JR, Auwerx J, Bruning JC, Chan L, Eckel RH, Farese RV, Jr, Galgani JE, Hambly C, Herman MA, Horvath TL, Kahn BB, Kozma SC, Maratos-Flier E, Muller TD, Munzberg H, Pfluger PT, Plum L, Reitman ML, Rahmouni K, Shulman GI, Thomas G, Kahn CR, Ravussin E.** 2012. A guide to analysis of mouse energy metabolism. Nat. Methods **9:**57–63. http://dx.doi.org/10.1038/nmeth.1806.
45. **Kiefer FW, Vernochet C, O'Brien P, Spoerl S, Brown JD, Nallamshetty S, Zeyda M, Stulnig TM, Cohen DE, Kahn CR, Plutzky J.** 2012. Retinaldehyde dehydrogenase 1 regulates a thermogenic program in white adipose tissue. Nat. Med. **18:**918–925. http://dx.doi.org/10.1038/nm.2757.
46. **Palanivel R, Fullerton MD, Galic S, Honeyman J, Hewitt KA, Jorgensen SB, Steinberg GR.** 2012. Reduced Socs3 expression in adipose tissue protects female mice against obesity-induced insulin resistance. Diabetologia **55:**3083–3093. http://dx.doi.org/10.1007/s00125-012-2665-3.
47. **Yang SJ, Xu CQ, Wu JW, Yang GS.** 2010. SOCS3 inhibits insulin signaling in porcine primary adipocytes. Mol. Cell. Biochem. **345:**45–52. http://dx.doi.org/10.1007/s11010-010-0558-7.
48. **Shi H, Tzameli I, Bjorbaek C, Flier JS.** 2004. Suppressor of cytokine signaling 3 is a physiological regulator of adipocyte insulin signaling. J. Biol. Chem. **279:**34733–34740. http://dx.doi.org/10.1074/jbc.M403886200.
49. **Alapatt P, Guo F, Komanetsky SM, Wang S, Cai J, Sargsyan A, Rodriguez Diaz E, Bacon BT, Aryal P, Graham TE.** 2013. Liver retinol transporter and receptor for serum retinol-binding protein (RBP4). J. Biol. Chem. **288:**1250–1265. http://dx.doi.org/10.1074/jbc.M112.369132.
50. **Yamada T, Katagiri H, Ishigaki Y, Ogihara T, Imai J, Uno K, Hasegawa Y, Gao J, Ishihara H, Niijima A, Mano H, Aburatani H, Asano T, Oka Y.** 2006. Signals from intra-abdominal fat modulate insulin and leptin sensitivity through different mechanisms: neuronal involvement in food-intake regulation. Cell Metab. **3:**223–229. http://dx.doi.org/10.1016/j.cmet.2006.02.001.
51. **Harms M, Seale P.** 2013. Brown and beige fat: development, function and therapeutic potential. Nat. Med. **19:**1252–1263. http://dx.doi.org/10.1038/nm.3361.
52. **Biddinger SB, Almind K, Miyazaki M, Kokkotou E, Ntambi JM, Kahn CR.** 2005. Effects of diet and genetic background on sterol regulatory element-binding protein-1c, stearoyl-CoA desaturase 1, and the development of the metabolic syndrome. Diabetes **54:**1314–1323. http://dx.doi.org/10.2337/diabetes.54.5.1314.
53. **Almind K, Kahn CR.** 2004. Genetic determinants of energy expenditure and insulin resistance in diet-induced obesity in mice. Diabetes **53:**3274–3285. http://dx.doi.org/10.2337/diabetes.53.12.3274.
54. **Vitali A, Murano I, Zingaretti MC, Frontini A, Ricquier D, Cinti S.** 2012. The adipose organ of obesity-prone C57BL/6J mice is composed of mixed white and brown adipocytes. J. Lipid Res. **53:**619–629. http://dx.doi.org/10.1194/jlr.M018846.
55. **Grove KL, Fried SK, Greenberg AS, Xiao XQ, Clegg DJ.** 2010. A microarray analysis of sexual dimorphism of adipose tissues in high-fat-diet-induced obese mice. Int. J. Obes. (Lond.) **34:**989–1000. http://dx.doi.org/10.1038/ijo.2010.12.
56. **Garcia-Barrado MJ, Iglesias-Osma MC, Moreno-Viedma V, Pastor Mansilla MF, Gonzalez SS, Carretero J, Moratinos J, Burks DJ.** 2011. Differential sensitivity to adrenergic stimulation underlies the sexual dimorphism in the development of diabetes caused by Irs-2 deficiency. Biochem. Pharmacol. **81:**279–288. http://dx.doi.org/10.1016/j.bcp.2010.10.008.
57. **Tiraby C, Tavernier G, Capel F, Mairal A, Crampes F, Rami J, Pujol C, Boutin JA, Langin D.** 2007. Resistance to high-fat-diet-induced obesity and sexual dimorphism in the metabolic responses of transgenic mice with moderate uncoupling protein 3 overexpression in glycolytic skeletal muscles. Diabetologia **50:**2190–2199. http://dx.doi.org/10.1007/s00125-007-0765-2.
58. **Yasmeen R, Reichert B, Deiuliis J, Yang F, Lynch A, Meyers J, Sharlach M, Shin S, Volz KS, Green KB, Lee K, Alder H, Duester G, Zechner R, Rajagopalan S, Ziouzenkova O.** 2013. Autocrine function of aldehyde dehydrogenase 1 as a determinant of diet- and sex-specific differences in visceral adiposity. Diabetes **62:**124–136. http://dx.doi.org/10.2337/db11-1779.
59. **Berry DC, Croniger CM, Ghyselinck NB, Noy N.** 2012. Transthyretin blocks retinol uptake and cell signaling by the holo-retinol-binding protein receptor STRA6. Mol. Cell. Biol. **32:**3851–3859. http://dx.doi.org/10.1128/MCB.00775-12.
60. **Carrera S, Cuadrado-Castano S, Samuel J, Jones GD, Villar E, Lee SW, Macip S.** 2013. Stra6, a retinoic acid-responsive gene, participates in p53-induced apoptosis after DNA damage. Cell Death Differ. **20:**910–919. http://dx.doi.org/10.1038/cdd.2013.14.
61. **Mcilroy GD, Delibegovic M, Owen C, Stoney PN, Shearer KD, McCaffery PJ, Mody N.** 2013. Fenretinide treatment prevents diet-induced obesity in association with major alterations in retinoid homeostatic gene expression in adipose, liver, and hypothalamus. Diabetes **62:**825–836. http://dx.doi.org/10.2337/db12-0458.
62. **Yahagi N, Shimano H, Matsuzaka T, Najima Y, Sekiya M, Nakagawa Y, Ide T, Tomita S, Okazaki H, Tamura Y, Iizuka Y, Ohashi K, Gotoda T, Nagai R, Kimura S, Ishibashi S, Osuga J, Yamada N.** 2003. p53 Activation in adipocytes of obese mice. J. Biol. Chem. **278:**25395–25400. http://dx.doi.org/10.1074/jbc.M302364200.
63. **Tsukamoto AS, Grosschedl R, Guzman RC, Parslow T, Varmus HE.** 1988. Expression of the int-1 gene in transgenic mice is associated with mammary gland hyperplasia and adenocarcinomas in male and female mice. Cell **55:**619–625. http://dx.doi.org/10.1016/0092-8674(88)90220-6.
64. **Shackleford GM, Varmus HE.** 1987. Expression of the proto-oncogene int-1 is restricted to postmeiotic male germ cells and the neural tube of mid-gestational embryos. Cell **50:**89–95. http://dx.doi.org/10.1016/0092-8674(87)90665-9.
65. **Mody N, Graham TE, Tsuji Y, Yang Q, Kahn BB.** 2008. Decreased clearance of serum retinol-binding protein and elevated levels of transthyretin in insulin-resistant ob/ob mice. Am. J. Physiol. Endocrinol. Metab. **294:**E785–E793. http://dx.doi.org/10.1152/ajpendo.00521.2007.
66. **Preitner F, Mody N, Graham TE, Peroni OD, Kahn BB.** 2009. Long-term fenretinide treatment prevents high-fat-diet-induced obesity, insulin resistance, and hepatic steatosis. Am. J. Physiol. Endocrinol. Metab. **297:**E1420–E1429. http://dx.doi.org/10.1152/ajpendo.00362.2009.
67. **Yu XX, Watts LM, Manchem P, Monia BP, Bhanot S.** 2008. Antisense reduction of retinol-binding protein 4 expression in liver and adipose tissues causes robust improvements in insulin sensitivity in diabetic and obese mice. Diabetes **57**(Suppl 1A)**:**LB21. http://professional.diabetes.org/Abstracts_Display.aspx?TYP=1&CID=71035.
68. **Moraes-Vieira PM, Yore MM, Dwyer PM, Syed I, Aryal P, Kahn BB.** RBP4 activates antigen-presenting cells leading to adipose tissue inflammation and systemic insulin resistance. Cell Metab., in press.
69. **Lumeng CN, Saltiel AR.** 2011. Inflammatory links between obesity and metabolic disease. J. Clin. Invest. **121:**2111–2117. http://dx.doi.org/10.1172/JCI57132.
70. **Deng ZB, Poliakov A, Hardy RW, Clements R, Liu C, Liu Y, Wang J, Xiang X, Zhang S, Zhuang X, Shah SV, Sun D, Michalek S, Grizzle WE, Garvey T, Mobley J, Zhang HG.** 2009. Adipose tissue exosome-like vesicles mediate activation of macrophage-induced insulin resistance. Diabetes **58:**2498–2505. http://dx.doi.org/10.2337/db09-0216.
71. **Amengual J, Golczak M, Palczewski K, von Lintig J.** 2012. Lecithin: retinol acyltransferase is critical for cellular uptake of vitamin A from serum retinol-binding protein. J. Biol. Chem. **287:**24216–24227. http://dx.doi.org/10.1074/jbc.M112.353979.
72. **Isken A, Golczak M, Oberhauser V, Hunzelmann S, Driever W, Imanishi Y, Palczewski K, von Lintig J.** 2008. RBP4 disrupts vitamin A uptake homeostasis in a STRA6-deficient animal model for Matthew-Wood syndrome. Cell Metab. **7:**258–268. http://dx.doi.org/10.1016/j.cmet.2008.01.009.
73. **Zolfaghari R, Ross AC.** 2002. Lecithin:retinol acyltransferase expression is regulated by dietary vitamin A and exogenous retinoic acid in the lung of adult rats. J. Nutr. **132:**1160–1164. http://jn.nutrition.org/content/132/6/1160.long.